Mapping the Transcriptome Underpinning Acute Corticosteroid Action within the Cortical Collecting Duct

Mapping the Transcriptome Underpinning Acute Corticosteroid Action within the Cortical Collecting Duct

Struan Loughlin[1,2], Hannah M. Costello[2], Andrew J. Roe[3], Charlotte Buckley[4], Stuart M. Wilson[3], Matthew A. Bailey[1] and Morag K. Mansley[1,2,3]

[1]Cellular Medicine Research Division, University of St Andrews, North Haugh, St Andrews, KY16 9TF, UK; [2]Centre for Cardiovascular Science, Queen's Medical Research Institute, The University of Edinburgh, Edinburgh, EH16 4TJ, UK; [3]Division of Pharmacy, School of Medicine, Pharmacy and Health, Durham University Queen's Campus, Stockton-on-Tees, TS17 6BH, UK; [4]Strathclyde Institute of Pharmacy and Biomedical Sciences, University of Strathclyde, Glasgow, G4 0RE, UK.

*Address for Correspondence: Dr Morag K. Mansley, [1]Cellular Medicine Research Division, University of St Andrews, North Haugh, St Andrews, KY16 9TF, UK. Email: mkm27@st-andrews.ac.uk

Key Points

- We report the transcriptomes associated with acute corticosteroid regulation of ENaC activity in polarised $mCCD_{cl1}$ collecting duct cells.
- 9 genes were regulated by aldosterone (ALDO), 0 with corticosterone alone and 151 with corticosterone when 11βHSD2 activity was inhibited.
- We validated 3 novel ALDO-induced genes: *Rasd1*, *Sult1d1* and *Gm43305* in primary cells isolated from a novel principal cell reporter mouse.

Abstract

Background

Corticosteroids regulate distal nephron and collecting duct Na^+ reabsorption, contributing to fluid-volume and blood pressure homeostasis. The transcriptional landscape underpinning the acute stimulation of the epithelial sodium channel (ENaC) by physiological concentrations of corticosteroids remains unclear.

Methods

Transcriptomic profiles underlying corticosteroid-stimulated ENaC activity in polarised $mCCD_{cl1}$ cells were generated by coupling electrophysiological measurements of amiloride-sensitive currents with RNAseq. Generation of a principal cell-specific reporter mouse line, mT/mG-Aqp2Cre, enabled isolation of primary collecting duct principal cells by FACS and ENaC activity was measured in cultured primary cells following acute application of corticosteroids. Expression of target genes was assessed by qRT-PCR in cultured cells or freshly isolated cells following acute elevation of steroid hormones in mT/mG-Aqp2Cre mice.

Results

Physiological relevance of the $mCCD_{cl1}$ model was confirmed with aldosterone-specific stimulation of SGK1 and ENaC activity. Corticosterone only modulated these responses at supraphysiological concentrations or when 11βHSD2 was inhibited. When 11βHSD2 protection was intact, corticosterone caused no significant change in transcripts. We identified a small number of aldosterone-induced transcripts associated with stimulated ENaC activity in $mCCD_{cl1}$ cells and a much larger number with corticosterone in the absence of 11βHSD2 activity. Principal cells isolated from mT/mG-Aqp2Cre mice were validated and assessment of identified aldosterone-induced genes revealed that *Sgk1*, *Zbtbt16*, *Sult1d1*, *Rasd1* and *Gm43305* are acutely upregulated by corticosteroids both *in vitro* and *in vivo*.

Conclusions

This study reports the transcriptome of $mCCD_{cl1}$ collecting duct cells and identifies a small number of aldosterone-induced genes associated with acute stimulation of ENaC, including 3 previously undescribed genes.

Introduction

Aldosterone (ALDO) and cortisol both influence blood pressure: ALDO as the final effector in the renin-angiotensin-aldosterone system (RAAS), promoting Na^+ reabsorption in the kidney; cortisol, in addition to being thought of as a "stress" hormone, being linked to the circadian rhythm of blood pressure. Within the kidney, ALDO acts specifically in the cells of the "aldosterone-sensitive distal nephron" (ASDN), where the mineralocorticoid receptor (MR) and the enzyme 11-beta-hydroxysteroid dehydrogenase type 2 (11βHSD2) are both expressed.[1] 11βHSD2 converts circulating cortisol to the inactive metabolite cortisone, conferring ALDO specificity to the ASDN which has previously been demarked as the late distal convoluted tubule (DCT2), connecting tubule (CNT) and collecting duct (CD).[1] There is now increasing evidence that 11βHSD2 is absent in the DCT,[2, 3] thus the boundaries of the ASDN may need updating to include the CNT and CCD only. Genetic mutations or pharmacological inhibition of 11βHSD2 cause hypertension in both humans[4] and rodents,[5] highlighting the importance of 11βHSD2 to blood pressure control. Additionally, recent evidence suggests that in states of glucocorticoid excess (e.g. chronic stress, obesity), cortisol may cause hypertension due to aberrant activation of renal sodium transport. Causal mechanisms are not fully understood but activation of the epithelial sodium channel (ENaC) *via* MR and the glucocorticoid receptor (GR) have been implicated.[6]

The classical actions of corticosteroids in the kidney involve hormones binding cytosolic steroid receptors within the epithelial cells lining the ASDN, modulating transcriptional processes and subsequent stimulation of Na^+ reabsorption.[7] This involves the transepithelial movement of Na^+ back to the circulation, firstly crossing the apical membrane *via* the epithelial Na^+ channel (ENaC) and subsequent extrusion across the basolateral membrane *via* the Na^+/K^+ ATP-ase. ENaC is rate-limiting in this process and is subject to regulation by a number of different hormones and bioactive factors.[8] Elucidation of the transcriptional targets of corticosteroid action in the kidney have involved many studies over the past two decades which have made use of a variety of model systems e.g. whole kidney homogenate, microdissected tubules,[9] primary cells isolated by FACS[10, 11] as well as a number of cell lines;[12-14] utilising ever-improving technology e.g. SAGE analysis, microarrays and more recently next generation sequencing. Key transcripts have been identified which encode target proteins including the serum and glucocorticoid-induced kinase 1 (SGK1) and the glucocorticoid-induced leucine zipper protein (GILZ), both of which have been shown to regulate ENaC activity.[15-17] However, there are discrepancies regarding the relative roles of these steroid-induced genes particularly considering the phenotypic difference in mice following nephron-specific deletion of MR[18] compared with deletion of e.g. SGK1[19] or GILZ.[20] Furthermore, the high concentrations of corticosteroids used to identify relevant genes in various model systems leaves the physiological relevance of these transcripts to steroid-induced ENaC activity within the distal nephron unclear.

The objective of this study was therefore to apply an unbiased, reductionist approach to generate transcriptomic profiles associated with the acute Na^+ retaining effects of corticosteroids in a physiologically relevant murine cell model of the cortical CD, $mCCD_{cl1}$ cells. These display many of the reported features of Na^+ absorbing principal cells of the collecting duct: predominant amiloride-sensitive Na^+ conductance *via* ENaC, a K^+ conductance mediated *via* the renal outer medullary K^+ channel (ROMK),[21] functional 11βHSD2 activity,[22] as well as regulation of these transport pathways by physiological concentrations of hormones including aldosterone and arginine vasopressin (AVP).[22, 23] We report the full transcriptome of the $mCCD_{cl1}$ cells and identify 9 ALDO-

induced genes. Lack of transcriptional effects of corticosterone (CORT) confirm 11βHSD2 activity, and upon pharmacological inhibition of this enzyme, CORT modulated 151 genes. Identified ALDO-induced genes were validated in $mCCD_{cl1}$ cells and subsequently in primary CD cells isolated from a newly generated mT/mG-Aqp2Cre reporter mouse. Identified ALDO-induced targets were subsequently measured in both cultured primary principal cells treated with steroids or from principal cells isolated directly from reporter mice following acute injection of corticosteroids. Our findings confirm both *Sgk1* and *Zbtb16* as acute ALDO-induced genes, and we further report *Rasd1*, *Sult1d1* and the unannotated *Gm43305* which encodes a lncRNA.

Methods

Culture of $mCCD_{cl1}$ cells

$mCCD_{cl1}$ cells (Prof. Bernard Rossier, University of Lausanne, Switzerland) were maintained in routine culture[22, 24] at 37°C and 5% CO_2, in phenol-red free DMEM/F12 media supplemented with FBS (2%), triiodothyronine (1 nmol/l), sodium selenite (5 ng/ml), insulin (5 µg/ml), transferrin (5 µg/ml), L-glutamine (200 mmol/l), penicillin (100 U/ml), streptomycin (100 µg/ml), dexamethasone (50 nmol/l) and EGF (10 ng/ml). Cells were used between passages 29-35. For experiments, cells were seeded onto 0.4 µm polyester filter membranes (Corning CoStar Snapwells) and grown for 9-11 days with media exchange every 2 days. 48 h before experimental protocols, media was replaced with DMEM/F12 media supplemented with charcoal-stripped media (2%), penicillin (100 U/ml) and streptomycin (100 µg/ml). For the final 24 h, media was replaced with DMEM/F12 with penicillin (100 U/ml) and streptomycin (100 µg/ml).

Quantification of transepithelial ion transport

Transepithelial voltage (V_{te}) and resistance (R_{te}) were measured using an epithelial volt-ohm-meter (EVOM) with chopstick "STX" electrodes (World Precision Instruments, Hertfordshire, UK). The equivalent short circuit current (I_{eq}) was subsequently calculated by Ohm's Law. V_{te} is shown relative to an earth electrode in the basolateral bath,[25] therefore a negative I_{eq} reflects either apical to basolateral movement of cations, basolateral to apical movement of anions or some combination of the two. Amiloride (10 µM, 10 min) was applied to the apical bath to determine the ENaC-mediated proportion of I_{eq}.

RNA sequencing

Total RNA was extracted from cells using the Rneasy kit (Qiagen) following electrophysiological measurements. RNA was subject to quality control (RNA ScreenTape) and RIN values were ≥9.0. TruSeq stranded mRNA-seq libraries were generated from each total RNA sample (24 libraries in total). Libraries were sequenced using the Illumina HiSeq 4000 Platform with 150 base pair paired-end reads. Reads were trimmed for quality (Cutadapt version 1.121) at the 3' end using a threshold of Q30 and for adapter sequences of the TruSeq stranded mRNA kit (AGATCGGAAGAGC) using Cutadapt version 1.121.[26] Reads after trimming were required to have a minimum length of 50. The raw RNAseq data have been uploaded to the Sequence Read Archive at NCBI, with the project ID: PRJNA820455. The reference used for mapping was the *Mus musculus* genome from Ensembl, assembly GRCm38, annotation version 84. Reads were aligned to the reference genome using STAR2 version 2.5.2b.[27] The raw counts table was filtered to remove rows consisting of predominantly near-zero counts (values had to be >0.05 across 5 samples), filtering on counts per million (CPM) to avoid artefacts due to library depth. Initial exploratory analysis indicated an outlier in the dataset, which was removed and subsequent filtering and normalisation performed again for downstream analysis. Following filtering, 17,962 genes remained. Differential analysis was carried out with EdgeR[28] (version 3.16.5) and compared all possible combinations from the 4 experimental conditions.

Generation of a principal cell-specific reporter mouse

Aqp2Cre mice[29] (The Jackson Laboratory , USA) were crossed with mT/mG (tdTomato-GFP) mice[30] (Prof. Neil Henderson, The University of Edinburgh, UK). Both mouse strains were on a C57BL/6 background. To ensure kidney-specific Cre expression, female AQP2-Cre mice were bred with male mT/mG mice; female offspring which were heterozygous for both AQP2-Cre and mT/mG were subsequently bred with male mice homozygous for mT/mG. Genotyping for AQP2-Cre was carried out using a forward primer 5'-CTCTGCAGGAACTGGTGCTGG-3' and reverse primer 5'-GCGAACATCTTCAGGTTCTGCGG-3'. Genotyping for mT/mG was carried out using the forward primer 5'-CTCTGCTGCCTCCTGGCTTCT-3' and reverse primers: wildtype 5-CGAGGCGGATCACAAGCAATA-3' and mutant 5'-TCAATGGGCGGGGGTCGTT-3'. Experiments were performed on male mice aged 10-30 weeks, under the authority of a UK Home Office Project License and following approval by the University's Animal Welfare and Ethical Review Board.

Isolation and culture of primary principal cells

Mice (wild-type, mT/mG$^{+/+}$- Aqp2Cre$^{-/-}$ and mT/mG$^{+/+}$- Aqp2Cre$^{+/-}$) were terminated by rising CO_2 and PBS injected into the left ventricle to remove blood. Kidneys were excised, decapsulated and stored in ice-cold PBS. Both kidneys were manually chopped into small pieces and then homogenised in gentleMACS^{TM} C Tubes (Miltenyi Biotec, Surrey, UK).[31] Digestion buffer contained: RPMI supplemented with Collagenase V (0.425 mg/ml), Collagenase D (0.625 mg/ml), Dispase II (1 mg/ml), DNase I (30 µg/ml), penicillin (100 U/ml) and streptomycin (100 µg/ml). Cellular suspensions were digested for 30 min at 37°C before a second dissociation in the gentleMACS^{TM} Dissociator. An equal volume of neutralisation buffer (PBS supplemented with FBS 2% vol/vol and EDTA 1 µM) was added and cell suspensions were passed sequentially through 100 µm, 70 µm and 40 µm cell strainers. Cells were pelleted by centrifugation and red cell lysis was carried out using red blood cell lysis buffer (Sigma, Dorset, UK). Cells were pelleted and resuspended in 1 ml neutralisation buffer.

Cells were analysed and sorted using either a BD FACS Aria II or BD FACS Aria Fusion cell sorter. 405 nm, 488 nm and 561 nm lasers were used for excitation of DAPI, GFP and tdTom, respectively. Wild-type C57BL/6 and mT/mG$^{+/+}$-Aqp2Cre$^{-/-}$ kidney samples were processed first to define gates before processing mT/mG$^{+/+}$-Aqp2Cre$^{+/-}$ samples. DAPI, at a final concentration of 0.1 ug/ml, was added to cells immediately prior to sorting. Cells were gated for a stable recording, singlets (plotting forward scatter area *vs.* height), cells (forward scatter area *vs.* side scatter area), live cells (DAPI *vs.* forward scatter area), followed by exclusive gates for both tdTom and GFP (Supplementary Figure 3). From the GFP gate, a further gate was added to remove autofluorescence events detected within that channel and a final gate to remove a mixed population of both tdTom and GFP. Cell sorting was performed with a 100 µm nozzle and due to the starting cell numbers and the relatively small percentage of GFP positive events, a yield sort followed by a purity sort was employed to optimise sort/time efficiency. For initial validation studies, 100,000 tdTom cells were collected and all possible GFP cells. Once the GFP population was validated, only GFP events were collected. Flow cytometry data was analysed using FCS Express 7 (De Novo Software, Pasadena, CA, USA).

For downstream experiments, GFP+ sorted cells were then either spun down, supernatant removed and RLTplus buffer added for RNA extraction or instead were directly plated onto gelatin-coated 12 well plates with complete media. Cells were maintained under identical conditions as those used for culture of $mCCD_{cl1}$ cells with the addition of gelatin coating of either the initial 12 well plate or the permeable membrane used for growing polarised monolayers.

Acute steroid treatment of mT/mG-Aqp2Cre mice

Male $mT/mG^{+/+}$-$Aqp2Cre^{+/-}$ mice, aged 10-30 weeks, were administered carbenoxolone (CBX) at 2.5mg/kg BW/day *po* (in drinking water) to inhibit endogenous 11βHSD2,[32] control animals were given *ad lib* access to drinking water for 8 days. Animals were weighed every morning (between 08:00-10:00) 5 days prior to CBX/control treatment and subsequently throughout. On day 9 at 08:30, mice were administered with a single dose of steroid: aldosterone (10 µg/kg BW),[33] corticosterone (CORT, 0.5 mg/kg BW) or solvent vehicle (5 % EtOH) *via ip* injection. After 3 h, mice were sacrificed by rising concentration of CO_2 and CD cells (GFP+) were then isolated by FACS.

Immunofluorescence imaging

Kidneys were decapsulated, bisected (left kidney: longitudinal section and right kidney: transverse section) and immersed in MeOH-free 4% PFA for 2 h at 4°C. Half kidneys were then washed twice with PBS, transferred to an 18% sucrose solution at 4°C overnight and then embedded in OCT, frozen and sectioned at 10 µm onto glass slides. Sections were permeabilised with 0.2% Triton X-100 for 10 min, blocked with 10% donkey serum for 1 h and subsequently washed with TBS-T (0.05% Tween 20). Sections were mounted in ProLong Diamond Antifade Mountant (Life Technologies, Paisley, UK) and imaged at 40X using a Zeiss AxioScan.Z1.

All images were processed using Fiji,[34] and the same process was applied to images from both $mT/mG^{+/+}$-$Aqp2Cre^{-/-}$ and $mT/mG^{+/+}$- $Aqp2Cre^{+/-}$ kidneys. Channels were split and a background subtraction (50 pixels) was performed on the 555 nm channel. For low magnification images, the 488 nm channel image was duplicated and a Gaussian blur (sigma = 10) applied. To separate the Cre-GFP signal from the tubule-generated autofluorescence, the blurred image was subtracted from the raw image and a threshold applied such that on the Cre-GFP remained (~0.04 %). This was used to generate a mask, which was changed to 16-bit and a Gaussian blur (sigma = 7) applied. This was used as the green channel, and the autofluorescence as the grey channel. For high magnification images, the 488 nm channel image was duplicated and a Gaussian blur (sigma = 3) applied. The blurred image was again subtracted from the raw image and a threshold applied such that on the Cre-GFP remained (~0.01%). This was used to generate a mask, which was changed to 16-bit and a Gaussian blur (sigma = 2) applied and used as the green channel.

qRT-PCR

Total RNA was extracted from cells, either grown as monolayers in culture on filter membranes or directly following FACS of CD cells, using a QIAGEN RNeasy Plus Micro Kit. The integrity of the RNA preparations was verified using the Agilent RNA 6000 Pico Kit and Agilent 2100 Bioanalyser, samples with RIN values <7.5 were excluded. cDNA was transcribed from total RNA using Applied Biosystems High Capacity cDNA Reverse

Transcription Kit (Life Technologies). For experiments using lysates from cells grown in culture, 500 ng RNA was used and cDNA was diluted 1:20 to correlate to the middle of the 7-point calibration curve generated from serial dilutions. For experiments using isolated primary CD cells from mT/mG-AQP2Cre mice, 1 ng RNA was used, as determined by the lowest yield across the samples. cDNA was diluted 1:10, also to correlate with the middle of the calibration curve. qRT-PCR was performed using a Roche Light-Cycler 480 II using a probe-based assay (Roche Universal Probe Library, Sigma, Dorset, UK). Primers were designed using the ProbeFinder software within the Roche Assay Design Centre. Samples were run in triplicate and only Cq values with a standard deviation >0.3 were excluded. A selection of reference genes (*Actb1, HPRT, Tbp* and *18S*) were tested and included if expression remained unaltered across all samples (Supplementary Figures 2, 4 and 5). Negative controls included reverse transcriptase negative, RNA negative and H_2O only.

Western analysis

Cells were washed with ice-cold PBS (x3), lysed in lysis buffer[25] and vortexed. Protein concentration was quantified by Bradford assay (BioRad, Hertfordshire, UK). Samples were prepared by adding a fixed mass of protein lysate to sample buffer, reducing and denaturing by heating at 95°C for 5 min in the presence of 2-mercaptoethanol. Samples were subsequently fractionated on 10% SDS polyacrylamide gels, transferred to PVDF membranes, blocked and probed with primary antibodies of interest and respective HRP-linked secondary antibodies. Primary antibodies against $Thr^{346/356/366}$-phosphorylated and total forms of the protein encoded by n-myc downstream regulated 1 (NDRG1), as well as total serum and glucocorticoid-regulated kinase 1 (SGK1) were purchased from the Dundee Protein Phosphorylation Unit, University of Dundee (Dundee, UK). The antibody against β-actin was from Sigma (Dorset, UK). Immunoreactive proteins were visualised by enhanced chemi-luminescence and quantified by densitometric measurements, as described previously.[35]

Data analysis

Data are expressed as mean±95% CI. For western blotting and qRT-PCR, due to uneven distribution of data expressed as fold-change, all data were log-transformed. All datasets were subject to normality testing (Shapiro-Wilks) followed by either parametric testing: unpaired t-test, one-way or two-way ANOVA or non-parametric testing: Mann-Whitney or Kruskall-Wallis, where appropriate. Post-hoc analysis was also carried out where appropriate, details of specific tests used are included in the figure legends.

Results

Modulation of ENaC and SGK1 activity by corticosteroids in $mCCD_{cl1}$ cells. Polarised $mCCD_{cl1}$ cells generated an average transepithelial voltage (V_{te}) of 22.8±11.3 mV and resistance R_{te} of 1.6±0.6 kΩ·cm^2, giving an average equivalent short-circuit current (I_{eq}) of 13.7±3.4 μA·cm^{-2} (n=144). I_{eq} reflects ENaC-mediated Na^+ transport as ~95% is inhibited by amiloride (10 μM).[24] Corticosterone (CORT) stimulated the amiloride-sensitive current ($I_{ami\text{-}3h}$) at concentrations ≥100 nM, consistent with endogenous activity of the "protective" 11βHSD2 (Figure 1Ai). Inhibiting 11βHSD2 with carbenoxolone (CBX, 10 μM, 30 min) revealed a concentration-dependent stimulation of ENaC-mediated Na^+ transport by CORT at concentrations ≥1 nM (Figure 1Ai). Baseline current was not altered in cells treated with CBX alone. Aldosterone (ALDO) also stimulated I_{ami} in a concentration-dependent manner; this was independent of CBX pre-treatment, consistent with ALDO not being a substrate for this enzyme (Figure 1Bi). CORT-induced Na^+ transport correlated with increased activity and expression of the protein serum and glucocorticoid induced kinase 1 (SGK1), Figure 1Aii and iii. SGK1 abundance under basal conditions is very low,[36] however there is clear activity of this kinase as per the basal levels of phosphorylation of specific residues in a downstream target NDRG1. Both SGK1 activity and expression were increased with ALDO (Figure 1Bii and iii).

Mapping the transcriptomes associated with acute corticosteroid stimulation of ENaC-mediated Na^+ transport. Polarised $mCCD_{cl1}$ cells were treated for 3 h with either solvent vehicle, ALDO (3 nM) or CORT (100 nM), the latter in the absence or presence of CBX (10 μM). Consistent with the concentration response assays ALDO, or CORT in the presence of CBX, stimulated I_{ami} compared to control whilst CORT in the absence of CBX did not alter I_{ami} (Figure 2A). cDNA libraries were generated across each of the 4 groups (n=6) which underwent 150 bp paired-end sequencing. Over 94% of trimmed reads were mapped to the genome and of those, 97.0–98.4% mapped as pairs.

Differential gene expression analysis compared all possible contrasts of experimental condition using thresholds of a minimum $\log_2$ fold change of 1 and a false discovery rate <0.05 (Table 1). Volcano plots were generated and show the differential expression of genes in cells treated with vehicle compared to ALDO, CORT or CBX+CORT (Figure 2B). 9 genes were identified in the ALDO group compared to the control group and 151 genes were differentially expressed in the CBX+CORT group compared to the control group (Figure 2B). Table 2 lists all transcripts regulated by ALDO and Table 3 lists the top 15 upregulated and all downregulated annotated genes in the CBX+CORT group. No transcripts were differentially expressed in the CORT group and this finding correlates with a lack of stimulated I_{ami}. All 9 transcripts differentially expressed in the ALDO *vs.* control group were also differentially expressed in the CBX+CORT group *vs.* control. The complete list of differentially regulated genes, as well as a counts table across the 4 experimental groups can be found in the supplementary excel file. Five of the genes identified (*Sgk1*, *Sult1d1*, *Gm43305*, *Rasd1* and *Zbtb16*) were subsequently validated by qRT-PCR in polarised $mCCD_{cl1}$ cells (Supplementary Figure S1). Cells were treated in similar manner: CORT (100 nM) or vehicle for 3 h, following pre-incubation with CBX (10 μM) or vehicle for 30 min, or treated with ALDO (3 nM) or vehicle for 3 h. Electrophysiological measurements to monitor ENaC activity were made prior to RNA extraction (data not shown).

Generation and validation of a principal cell-specific reporter mouse. The mT/mG mouse line,[30] which ubiquitously express tdTomato (tdTom) in cell membranes (mT) or upon Cre excision express enhanced GFP (mG), was crossed with the Aqp2Cre line.[29] Fixed longitudinal sections of kidneys from adult offspring were imaged for tdTom and GFP labelling. mT/mG positive and Aqp2Cre null mice e.g. mT/mG$^{+/+}$-Aqp2Cre$^{-/-}$, demonstrated membrane labelling of tdTom in both cortex and medullary regions (Figure 3Ai). Distinct differences in labelling can be seen in the cortex where brush border membranes of the proximal tubules exhibit less evenly distributed membrane-associated markers than distal tubules and collecting ducts (Figure 3Aii). This is consistent with the expression pattern previously reported in kidney tissue.[29] Negligible eGFP labelling was detected (Figure 3Aiii). Kidney sections from adult mice homozygous for mT/mG and hemizygous for Aqp2Cre, e.g. mT/mG$^{+/+}$-Aqp2Cre$^{+/-}$ mice (B), displayed both tdTom and Cre-induced eGFP labelling in the cortex and medulla (Figure 3Bi-iii). The eGFP labelling of tubules is low, possibly indicating low recombination efficiency of the Aqp2Cre line, in our hands.

Expression of nephron segment-specific markers were determined in tdTom and GFP+ populations (Table 4). Whilst the tdTom population was enriched for markers consistent with the proximal tubule (NHE3) and the loop of Henle (NKCC2), the GFP+ population was enriched for markers of the CD. In particular, principal cell markers ROMK, α-ENaC and 11βHSD2, but also β-intercalated cell markers V-ATPase β1 and pendrin, but not the α-intercalated cell marker AE1 (Table 4). NCC expression was detected in both populations.

To determine functional properties, one isolated population was grown in culture over several weeks. Cells were subsequently seeded onto permeable inserts; after 9-11 days baseline V_{te} and R_{te} were -20.3±3.1 mV and 5.1±0.1 kΩ·cm^2 respectively, giving rise to an I_{eq} of -3.9±0.6 μA·cm^{-2} (values are mean±95% CI, n=25). It was noted that over numerous passages V_{te} reduced, R_{te} increased, thus I_{eq} decreased (data not shown). Cells were therefore used between passages 4-8 for all experiments. Similar to the mCCD$_{cl1}$ cells, application of amiloride (10 μM, 10 min) inhibited basal I_{eq} to negligible values (Figure 5A), indicating a predominant amiloride-sensitive current in the primary principal cells. A concentration response assay to CORT±CBX revealed that CORT stimulated $I_{ami\text{-}3h}$ at concentrations >100 nM and pre-incubating primary principal cells with CBX (10 μM, 30 min) unveiled a concentration-dependent stimulation of $I_{ami\text{-}3h}$ (Figure 4Ai). Stimulation of ENaC-mediated Na^+ transport correlated with increased activity of SGK1 activity, as determined by phosphorylation of NDRG1-Thr$^{346/356/366}$ (Figure 4Aii).

Corticosteroid regulation of ENaC activity and identified ALDO-induced genes in cultured primary principal cells. Primary principal cells were treated (3 h) with: CORT (10 nM) in the absence/presence of CBX (10 μM, 30 min pre-incubation), ALDO (3 nM) or dexamethasone (DEX, 100 nM). Consistent with the concentration response assays, CORT only stimulated $I_{ami\text{-}3h}$ when cells were pre-incubated with CBX: 2.4±0.3 fold vs. without CBX: 1.2±0.2 fold (Figure 5A, n=8). Both ALDO and DEX stimulated $I_{ami\text{-}3h}$ by 2.0±0.3 fold (Figure 5B, n = 8) and 3.6±fold (Fig 5C, n=8), respectively. Of the 8 targets tested: *Sgk1*, *Sult1d1*, *Gm43305*, *Rasd1*, *Zbtb16*, *Defb1*, *Gm16178* and *Gm9694*, expression of three were upregulated by CBX+CORT (10 nM) – *Sgk1*, *Gm43305* and *Zbtb16*. No targets were altered either by CORT or CBX alone (Figure 6). In cells treated with ALDO, expression of 3 out of 8 target transcripts tested was increased: *Sgk1*, *Rasd1* and *Zbtb16* (Figure 7A). Finally, in cells treated with DEX, all but one target tested (*Gm9694*) was upregulated (Figure 7B).

Corticosteroid regulation of identified ALDO-induced genes in principal cells isolated from mT/mG-Aqp2Cre mice. We measured expression of 6 ALDO-induced targets: *Sgk1*, *Sult1d1*, *Gm43305*, *Rasd1*, *Zbtb16*, and *Defb1* in isolated primary principal cells following acute treatment with steroid hormones or respective controls. Of these, 4 were upregulated in mice treated with ALDO: *Sult1d1*, *Gm43305*, *Rasd1*, *Zbtb16* (Figure 8A). These 4 transcripts were also upregulated in mice treated with CBX+CORT. Notably *Sult1d1*, *Gm43305* and *Zbtb16* were also upregulated in the CORT group but also in the CBX group.

Discussion

We have mapped the transcriptomes underlying corticosteroid-regulated ENaC activity, identifying a small number of ALDO-regulated genes and larger number of CORT-regulated genes, the latter only when 11βHSD2 was inhibited. We utilised mouse $mCCD_{cl1}$ cells,[22] a well-described model of ASDN to couple transcriptomic with electrophysiological analysis. ENaC activity was stimulated by low nanomolar concentrations of ALDO[22, 37] and by CORT at concentrations greater than 100 nM or when endogenous 11βHSD2 activity was inhibited by CBX. The "gatekeeping" activity of this enzyme extends to complete absence of transcriptional activity by CORT. Isolation of primary principal cells from a novel reporter mouse enabled assessment of steroid-induced ion transport and target gene expression, the latter both *in vitro* and *in vivo*.

Deep sequencing of polarised $mCCD_{cl1}$ cells revealed expression of genes associated with principal cells of CCD including: *Aqp2* (AQP2), *Hsd11b2* (11β-HSD2), *Kcnj1* (ROMK), *Kcnj10* (Kir4.1), *Nr3c1* (GR), *Nr3c2* (MR), *Scnn1a* (α-ENaC), *Scnn1b* (β-ENaC), *Scnn1g* (γ-ENaC). With low expression of *Slc12a3* (NCC) and absence of *Pvalb* (parvalbumin), *Slc12a1* (NKCC2) and *Slc9a3* (NHE3), these cells likely represent epithelia from DCT2 onwards. Whilst there is low expression of *Atp6v1b1* (V-ATPase β1), there is no detectable expression of either *Slc4a1* (AE1) or *Slc26a4* (pendrin), thus it seems $mCCD_{cl1}$ cells reflect a principal cell population. This expression profile aligns with principal cell populations identified by scSeq of mouse kidney.[38, 39] Transcriptomic profiling of the related cell line, $mpkCCD_{cl4}$,[40] revealed a similar pattern of transcripts, with the exception of *Kcnj1*, *Kcnj10* and *Nr3c2*.[41] More recently, RNAseq analysis of a subclone of these cells, $mpkCCD_{cl1}$, whilst also having a similar pattern of transcripts, revealed low expression of *Nr3c2*, but *Kcnj1*, *Kcnj10*, *Kcnj16* and *Scnn1b* were absent.[42] Functionally the $mpkCCD_{cl4}$ cell line does not exhibit ALDO-sensitivity, requiring micromolar concentrations to exert a stimulatory effect on ENaC,[40, 43, 44] consistent with the lack of, or very low abundance of, the MR.

We confirm both *Sgk1* and *Zbtb16* as early ALDO-induced genes,[16, 33, 45, 46] and further identify *Rasd1*, *Sult1d1* and an unannotated transcript *Gm43305*. SGK1 is well described as a steroid-induced protein which prevents ubiquitin-mediated removal of ENaC in the apical membrane through phosphorylation of the ubiquitin-ligase Nedd4-2.[47] *Zbtb16*, the promyelocytic leukaemia zinc finger protein (PLZF), was identified as an early ALDO-induced gene in M1 cells expressing rat MR.[46] Overexpression of PLZF reduced basal I_{SC} but did not alter dexamethasone-induced I_{SC}, suggesting that rather than mediating the stimulatory response of ALDO, PLZF may negatively regulate ENaC in the CD.[46] Whilst *Rasd1* has not been directly linked to corticosteroid effects in the CD, it has previously been identified as a downregulated transcript in SAGE analysis of the outer medullary collecting duct (OMCD) in mice following 3 days of K^+ depletion.[48] *Rasd1* has been identified as an intercalated cell-enriched transcript in mice.[49] Due to the potential plasticity of CD cells, or the de-differentiation of isolated cells, it will be prudent to determine in which cell-type Rasd1 is expressed *in vivo* and whether its induction by ALDO relates to ENaC stimulation. It is of note that a related gene from the Ras superfamily: *Kras* (also known as *KRas2a)* was previously identified as a steroid-induced transcript in amphibian A6 cells[50] and when co-expressed with ENaC in oocytes, stimulated amiloride-sensitive currents.[51] Whilst our data show expression of *Kras*, we did not detect significant changes in expression with any steroid treatment tested. *Sult1d1* was also upregulated by ALDO and two other family members *Sult1a1* and *Sult1b1* were upregulated in cells treated with CBX+CORT. Sulfonation has been associated with inactivation of molecules to facilitate excretion,[52] and it may also regulate intracellular bioavailability.[53] SULT1D1 has been associated with catecholamine sulfation in mouse kidney, thought to enhance excretion.[54] However, with no human orthologue of *Sult1d1*, it may represent a species-dependent regulation of catecholamines. Finally, *Gm43305* is an unannotated transcript encoding a long non-coding RNA located upstream of the olfactory receptor *Olfr49* on chromosome 14. Whether this ALDO-induced lncRNA relates to the stimulation of ENaC remains unknown, but it is of interest whether lncRNAs may be identified as yet another layer of regulation of ion transport processes in the distal nephron.

We compared acute ALDO-induced transcriptional events from this study with two recent studies which mapped the transcriptomes of isolated primary cells of the ASDN following chronic ALDO treatment.[10, 11] In these 2 studies, mice kept on a low Na^+ diet for 5 days or infused with exogenous ALDO by osmotic minipump for 6 days, had plasma [ALDO] of ~ 1.5 nM, which is comparable to the 3 nM used in our own study. Of the ALDO-induced genes identified in the present study, both *Sult1d1* and/or *Sgk1* were identified as aldosterone-regulated.[10, 11] From the full transcriptome of the DCT/CNT/iCCD under control conditions,[10] expression of 7 out of 9 of our ALDO-induced transcripts were detected, with the absence of 2 identified unannotated genes *Gm43305* and *Gm9694*. The differences in ALDO-induced genes between our study and these others may reflect the acute time-frame in which we measured transcriptional changes and may align with the concept of early *vs.* late effects of ALDO in the ASDN.[55]

ENaC-mediated Na^+ transport in the ASDN is not normally responsive to CORT due to 11βHSD2 activity.[56, 57] We confirmed ENaC cannot be stimulated by CORT at physiological concentrations in $mCCD_{cl1}$ cells[22] and subsequently demonstrated SGK1 expression/activity is also protected. Our transcriptomic data reveal that 11βHSD2, in fact, fully abolishes the transcriptional effects of CORT and since no 11βHSD1 expression was detected, CORT is fully inactivated and cannot be re-activated in principal cells. Recent work suggests that the ASDN may in fact not include the late DCT/early CNT, where basal ENaC activity is much greater than in the CNT/CCD.[58] Dietary manoeuvres which raise plasma [ALDO] produce different effects on ENaC depending on its location. Whilst ENaC activity is stimulated in both the DCT/CNT and CNT/CCD in mice maintained on a high K^+ diet,[59] ENaC activity is only stimulated in the CNT/CCD in mice maintained on a low Na^+ diet.[60] The MR, appears critical in both regions for steroid-induced ENaC activity as deletion abolishes these responses.[59, 61] It is interesting to speculate whether expression of the cellular machinery underpinning ALDO sensitivity differs in these locations giving rise to different basal, as well as ALDO-induced, ENaC activity. There are mixed reports regarding immunolocalization of 11βHSD2 in the DCT[2, 3, 62] and recent scSeq of murine kidneys report low/negligible expression.[38, 39, 63] We determined the transcriptomic effects of CORT in the absence of 11βHSD2: ENaC activity was robustly stimulated and differential gene expression analysis revealed modulation of a much larger number of genes compared to ALDO, including previously described steroid-induced targets: GILZ, α-ENaC, and Per1.[12, 13] All genes identified following ALDO treatment were identified in cells treated with CBX+CORT, indicating a shared pathway of these hormones downstream of binding endogenous receptors. The relative roles that the MR, GR or indeed both within the distal nephron, particularly where 11βHSD2 is absent *vs.* present remains incompletely understood and warrants further investigation.

Generating mT/mG-Aqp2Cre mice to isolate primary CD cells is a similar strategy to previous studies that utilised a TRPV5-eGFP reporter line to isolate primary CNT/CD cells[10] or CD-specific cell isolation from wild-type mice using either DBA lectin[64] or an L1-CAM antibody.[11] In our study, the isolated GFP+ cells were, as expected, strongly enriched for genes characteristic of principal cells (encoding 11βHSD2, ROMK, α-ENaC). These cells also expressed genes encoding pendrin and AE1, associated with intercalated cells, albeit at a low abundance. This finding is consistent with groups who isolated primary CD cells[11] or DCT2/CNT/initial CCD cells.[10] We do not think our results reflect non-specificity of Cre-recombinase as Aqp2Cre is not expressed in intercalated cells.[29] Nor do we consider this to be contamination during isolation e.g. due to autofluorescence: our gating strategy was stringent and we did not detect enrichment of markers associated with proximal tubule cells, which exhibit strong autofluorescence. It is possible that either the isolated primary principal cells de-differentiate rapidly or perhaps more likely, our results support the evidence that CD epithelia exhibit plasticity.[38, 65, 66] Indeed, scSeq analysis of murine kidney[38] reported a "transitional cell" type where high expression of these IC transcripts were detected, at a similar level as *Aqp2*. The finding that the GFP+ cells contain transcripts associated with PCs but also ICs is consistent with this. Importantly, functional assessment of the isolated GFP+ cells revealed 11βHSD2 activity as well as predominant amiloride-sensitive currents which could be stimulated by aldosterone, therefore the isolated GFP+ cells phenotypically behave as Na^+ absorbing principal cells.

Primary principal cells grown on permeable supports in culture developed V_t and R_t in a manner analogous to $mCCD_{cl1}$ cells. R_t, of note, was much larger in these cells at ~ 5 kΩ·cm^2, with a V_t of ~ -20 mV giving rise to an I_{eq} of ~ -3.5 μA·cm^{-2}. These currents are smaller than those recorded from $mCCD_{cl1}$,[22, 24] $mpkCCD_{cl4}$,[35, 40] as well as primary CD cells isolated by DBA lectin,[64] but were almost completely abolished by amiloride indicating a Na^+ absorbing phenotype *via* ENaC. Primary principal cells exhibited 11βHSD2 activity and ENaC-mediated currents were significantly stimulated by ALDO, CBX+CORT, as well as dexamethasone (DEX). This correlates with currents measured in $mCCD_{cl1}$ cells, confirming these cells represent a relevant model of principal cells with the advantage that they do not de-differentiate over a small number of passages. Analysis of identified ALDO-induced genes in primary cells grown in culture revealed ALDO and CBX+CORT both upregulated *Sgk1*, *Rasd1* and *Zbtb16*, but ALDO also upregulated *Sult1d1* whereas CORT also upregulated *Gm43305*. Interestingly, DEX upregulated 7 of 8 ALDO-induced genes tested. Studies have shown that whilst DEX is considered a synthetic glucocorticoid, it can bind the MR as well as the GR.[67] In the transcriptomic data from the $mCCD_{cl1}$ cells, MR is expressed at 4x greater levels than GR, smaller than the 7x difference reported in the $mpkCCD_{cl1}$ cells,[42] but similar to the 3x greater levels reported in the CD principal cell population identified in scSeq analysis of murine kidney.[38]

Building on our *in vitro* experiments, principal cell-specific reporter mice were acutely administered ALDO or CORT±CBX.[68] Four of the identified ALDO-induced genes were upregulated in mice treated with either ALDO or CBX+CORT: *Sult1d1*, *Gm443305*, *Rasd1* and *Zbtb16*. We noted that CBX treatment alone resulted in an upregulation in expression of the ALDO-induced genes *Zbtb16*, *Gm43305* and *Sult1d1*. We did not, however, detect changes in *Sgk1* across any of the groups. *Sgk1* has previously been shown to be upregulated in microdissected CNT/CCD following 1 h ALDO treatment[33] and it is possible these rapid activation events were complete by our 3 h collection point. However, from the data, it is clear that four of our identified corticosteroid-induced genes remained upregulated after 3 h.

In summary, we report the transcriptional landscape associated with acute corticosteroid-induced ENaC activity in principal cells of the CD. In addition to the previously described ALDO-induced targets *Sgk1* and *Zbtb16*, we identify 3 additional acutely upregulated targets *Rasd1*, *Sult1d1* and the unannotated *Gm43305*. The potential role that these genes play in mediating ALDO- induced ENaC activity in principal cells of the CD is of interest and remains to be determined.

Disclosures

M. Bailey reports the following: Consultancy: River 2 Renal; and Advisory or Leadership Role: Kidney Research UK (Research Grant & Fellowships Committee); American Journal of Physiology (Associate Editor). S. Wilson reports the following: Ownership Interest: Diageo; Legal & General Group; Reckitt Benckiser Group Plc; Unilever Plc; Astra Zeneca PLC. The remaining authors have nothing to disclose.

Funding

This was work supported by Kidney Research UK: a Postdoctoral Fellowship PDF_008_20151127 and Innovation Grant IN_001_20170302; the British Heart Foundation: Research Excellence Award RE/13/3/30183; The Scottish Funding Council: St Andrews Research Funding Scheme; and the Society for Endocrinology: Early Career Grant.

Acknowledgements

The authors are grateful to Dr. Laura Denby and Carolynn Cairns within the Centre for Cardiovascular Science for giving guidance in preparing kidney homogenates for FACS. We thank Prof. Neil Henderson at The University of Edinburgh for access to the mT/mG reporter mouse and guidance on breeding/genotyping strategies. We are grateful to Dr. Shonna Johnston and the Flow CoRE facility in the QMRI for their expertise and guidance for FACS experiments. Finally, the authors acknowledge the services of Edinburgh Genomics, as well as Dr. Peter Thorpe at the University of St Andrews for bioinformatics support.

Author Contributions

M.K.M. and M.A.B. conception and design of research; M.K.M., S.R.L., A.R. and H.M.C. performed experiments; M.K.M., S.R.L., H.M.C., A.R. and C.B. analysed the data; M.K.M. prepared figures; M.K.M. drafted the manuscript; M.K.M. and M.A.B. edited and revised manuscript; M.K.M., S.R.L., H.M.C., A.R., C.B., S.M.W. and M.A.B. approved final version of the manuscript.

Data sharing statement

The raw RNAseq data have been uploaded to the Sequence Read Archive at NCBI, with the project ID: PRJNA820455.

Supplemental Material

References

1. Loffing J, Korbmacher C: Regulated sodium transport in the renal connecting tubule (CNT) via the epithelial sodium channel (ENaC). *Pflugers Archiv European Journal of Physiology,* 458**:** 111-135, 2009

2. Hunter RW, Ivy JR, Flatman PW, Kenyon CJ, Craigie E, Mullins LJ*, et al.*: Hypertrophy in the distal convoluted tubule of an 11b-hydroxysteroid dehydrogenase type 2 knockout model. *Journal of the American Society of Nephrology,* 26**:** 1537-1548, 2015

3. Maeoka Y, Su XT, Wang WH, Duan XP, Sharma A, Li N*, et al.*: Mineralocorticoid Receptor Antagonists Cause Natriuresis in the Absence of Aldosterone. *Hypertension,* 79**:** 1423-1434, 2022

4. Stewart PM, Corrie JET, Shackleton CHL, Edwards CRW: Syndrome of apparent mineralocorticoid excess - a defect in the cortisol cortisone shuttle. *Journal of Clinical Investigation,* 82**:** 340-349, 1988

5. Kotelevtsev Y, Brown RW, Fleming S, Kenyon C, Edwards CRW, Seckl JR*, et al.*: Hypertension in mice lacking 11 beta-hydroxysteroid dehydrogenase type 2. *Journal of Clinical Investigation,* 103**:** 683-689, 1999

6. Hunter R, Ivy JR, Bailey MA: Glucocorticoids and renal Na^+ transport: implications for hypertension and salt sensitivity. *Journal of Physiology,* 592**:** 1731-1744, 2014

7. Verrey F: Transcriptional control of sodium transport in tight epithelia by adrenal steroids. *Journal of Membrane Biology,* 144**:** 93-110, 1995

8. Shane MA, Nofziger C, Blazer-Yost BL: Hormonal regulation of the epithelial Na^+ channel: From amphibians to mammals. *General and Comparative Endocrinology,* 147**:** 85-92, 2006

9. Muller OG, Parnova RG, Centeno G, Rossier BC, Firsov D, Horisberger JD: Mineralocorticoid effects in the kidney: Correlation between aENaC, GILZ, and Sgk-1 mRNA expression and urinary excretion of Na^+ and K^+. *Journal of the American Society of Nephrology,* 14**:** 1107-1115, 2003

10. Poulsen SB, Limbutara K, Fenton RA, Pisitkun T, Christensen BM: RNA sequencing of kidney distal tubule cells reveals multiple mediators of chronic aldosterone action. *Physiological Genomics,* 50**:** 343-354, 2018

11. Swanson EA, Nelson JW, Jeng S, Erspamer KJ, Yang CL, McWeeney S*, et al.*: Salt-sensitive transcriptome of isolated kidney distal tubule cells. *Physiological Genomics,* 51**:** 125-135, 2019

12. Robert-Nicoud M, Flahaut M, Elalouf JM, Nicod M, Salinas M, Bens M*, et al.*: Transcriptome of a mouse kidney cortical collecting duct cell line: Effects of aldosterone and vasopressin. *Proceedings of the National Academy of Sciences of the United States of America,* 98**:** 2712-2716, 2001

13. Gumz ML, Popp MP, Wingo CS, Cain BD: Early transcriptional effects of aldosterone in a mouse inner medullary collecting duct cell line. *American Journal of Physiology-Renal Physiology,* 285**:** F664-F673, 2003

14. Gonzalez-Nunez D, Morales-Ruiz M, Leivas A, Hebert SC, Poch E: In vitro characterization of aldosterone and cAMP effects in mouse distal convoluted tubule cells. *American Journal of Physiology - Renal Physiology,* 286**:** F936-F944, 2004

15. Alvarez De La Rosa D, Zhang P, Náray-Fejes-Tóth A, Fejes-Tóth G, Canessa CM: The serum and glucocorticoid kinase sgk increases the abundance of epithelial sodium channels in the plasma membrane of Xenopus oocytes. *Journal of Biological Chemistry,* 274**:** 37834-37839, 1999

16. Chen SY, Bhargava A, Mastroberardino L, Meijer OC, Wang J, Buse P*, et al.*: Epithelial sodium channel regulated by aldosterone-induced protein sgk. *Proceedings of the National Academy of Sciences of the United States of America,* 96**:** 2514-2519, 1999

17. Soundararajan R, Zhang TT, Wang J, Vandewalle A, Pearce D: A novel role for glucocorticoid-induced leucine zipper protein in epithelial sodium channel-mediated sodium transport. *Journal of Biological Chemistry,* 280**:** 39970-39981, 2005

18. Canonica J, Sergi C, Maillard M, Klusonova P, Odermatt A, Koesters R*, et al.*: Adult nephron-specific MR-deficient mice develop a severe renal PHA-1 phenotype. *Pflugers Archiv European Journal of Physiology,* 468**:** 895-908, 2016

19. Faresse N, Lagnaz D, Debonneville A, Ismailji A, Maillard M, Fejes-Toth G*, et al.*: Inducible kidney-specific Sgk1 knockout mice show a salt-losing phenotype. *American Journal of Physiology - Renal Physiology,* 302**:** F977-F985, 2012

20. Rashmi P, Colussi G, Ng M, Wu X, Kidwai A, Pearce D: Glucocorticoid-induced leucine zipper protein regulates sodium and potassium balance in the distal nephron. *Kidney International,* 91**:** 1159-1177, 2017

21. Fodstad H, Gonzalez-Rodriguez E, Bron S, Gaeggeler H, Guisan B, Rossier BC*, et al.*: Effects of mineralocorticoid and K^+ concentration on K^+ secretion and ROMK channel expression in a mouse cortical collecting duct cell line. *American Journal of Physiology - Renal Physiology,* 296**:** F966-F975, 2009

22. Gaeggeler HP, Gonzalez-Rodriguez E, Jaeger NF, Loffing-Cueni D, Norregaard R, Loffing J*, et al.*: Mineralocorticoid versus glucocorticoid receptor occupancy mediating aldosterone-stimulated sodium transport in a novel renal cell line. *Journal of the American Society of Nephrology,* 16**:** 878-891, 2005

23. Gaeggeler HP, Guillod Y, Loffing-Cueni D, Loffing J, Rossier BC: Vasopressin-dependent coupling between sodium transport and water flow in a mouse cortical collecting duct cell line. *Kidney International,* 79**:** 843-852, 2010

24. Mansley MK, Neuhuber W, Korbmacher C, Bertog M: Norepinephrine stimulates the epithelial Na^+ channel in cortical collecting duct cells via a_2-adrenoceptors. *American Journal of Physiology - Renal Physiology,* 308**:** F450-F458, 2015

25. Mansley MK, Wilson SM: Effects of nominally selective inhibitors of the kinases PI3K, SGK1 and PKB on the insulin-dependent control of epithelial Na^+ absorption. *British Journal of Pharmacology,* 161**:** 571-588, 2010

26. Martin M: Cutadapt removes adapter sequences from high-throughput sequencing reads. *2011,* 17**:** 3, 2011

27. Dobin A, Davis CA, Schlesinger F, Drenkow J, Zaleski C, Jha S*, et al.*: STAR: ultrafast universal RNA-seq aligner. *Bioinformatics,* 29**:** 15-21, 2013

28. Robinson MD, McCarthy DJ, Smyth GK: edgeR: a Bioconductor package for differential expression analysis of digital gene expression data. *Bioinformatics,* 26**:** 139-140, 2010

29. Nelson RD, Stricklett P, Gustafson C, Stevens A, Ausiello D, Brown D*, et al.*: Expression of an AQP2 Cre recombinase transgene in kidney and male reproductive system of transgenic mice. *American Journal of Physiology - Cell Physiology,* 275**:** C216-C226, 1998

30. Muzumdar MD, Tasic B, Miyamichi K, Li L, Luo LQ: A global double-fluorescent cre reporter mouse. *Genesis,* 45**:** 593-605, 2007

31. O'Sullivan J, Finnie SL, Teenan O, Cairns C, Boyd A, Bailey MA*, et al.*: Refining the mouse subtotal nephrectomy in male 129S2/SV mice for consistent modeling of progressive kidney disease with renal inflammation and cardiac dysfunction. *Frontiers in Physiology,* 10, 2019

32. Young MJ, Morgan J, Brolin K, Fuller PJ, Funder JW: Activation of mineralocorticoid receptors by exogenous glucocorticoids and the development of cardiovascular inflammatory responses in adrenalectomized rats. *Endocrinology,* 151**:** 2622-2628, 2010

33. Fakitsas P, Adam G, Daidié D, Van Bemmelen MX, Fouladkou F, Patrignani A*, et al.*: Early aldosterone-induced gene product regulates the epithelial sodium channel by deubiquitylation. *Journal of the American Society of Nephrology,* 18**:** 1084-1092, 2007

34. Schindelin J, Arganda-Carreras I, Frise E, Kaynig V, Longair M, Pietzsch T*, et al.*: Fiji: an open-source platform for biological-image analysis. *Nat Methods,* 9**:** 676-682, 2012

35. Mansley MK, Roe AJ, Francis SL, Gill JH, Bailey MA, Wilson SM: Trichostatin A blocks aldosterone-induced Na^+ transport and control of serum- and glucocorticoid-inducible kinase 1 in cortical collecting duct cells. *British Journal of Pharmacology,* 176**:** 4708-4719, 2019

36. Mansley MK, Watt GB, Francis SL, Walker DJ, Land SC, Bailey MA*, et al.*: Dexamethasone and insulin activate serum and glucocorticoid-inducible kinase 1 (SGK1) via different molecular mechanisms in cortical collecting duct cells. *Physiological Reports,* 4**:** e12792, 2016

37. Mansley MK, Korbmacher C, Bertog M: Inhibitors of the proteasome stimulate the epithelial sodium channel (ENaC) through SGK1 and mimic the effect of aldosterone. *Pflugers Arch,* 470**:** 295-304, 2018

38. Park J, Shrestha R, Qiu CX, Kondo A, Huang SZ, Werth M*, et al.*: Single-cell transcriptomics of the mouse kidney reveals potential cellular targets of kidney disease. *Science,* 360**:** 758-763, 2018

39. Ransick A, Lindstrom NO, Liu J, Zhu Q, Guo JJ, Alvarado GF*, et al.*: Single-cell profiling reveals sex, lineage, and regional diversity in the mouse kidney. *Developmental Cell,* 51**:** 399-413, 2019

40. Bens M, Vallet V, Cluzeaud F, Pascual-Letallec L, Kahn A, Rafestin-Oblin ME*, et al.*: Corticosteroid-dependent sodium transport in a novel immortalized mouse collecting duct principal cell line. *Journal of the American Society of Nephrology,* 10**:** 923-934, 1999

41. Yu MJ, Miller RL, Uawithya P, Rinschen MM, Khositseth S, Braucht DWW*, et al.*: Systems-level analysis of cell-specific AQP2 gene expression in renal collecting duct. *Proceedings of the National Academy of Sciences of the United States of America,* 106**:** 2441-2446, 2009

42. Isobe K, Jung HJ, Yang CR, Claxton J, Sandoval P, Burg MB*, et al.*: Systems-level identification of PKA-dependent signaling in epithelial cells. *Proceedings of the National Academy of Sciences of the United States of America,* 114**:** E8875-E8884, 2017

43. Flores SY, Loffing-Cueni D, Kamynina E, Daidié D, Gerbex C, Chabanel S*, et al.*: Aldosterone-induced serum and glucocorticoid-induced kinase 1 expression is accompanied by Nedd4-2 phosphorylation and increased Na^+ transport in cortical collecting duct cells. *Journal of the American Society of Nephrology,* 16**:** 2279-2287, 2005

44. Auberson M, Hoffman-Pochon N, Vandewalle A, Kellenberger S, Schild L: Epithelial Na^+ channel mutants causing Liddle's syndrome retain ability to respond to aldosterone and vasopressin. *American Journal of Physiology - Renal Physiology,* 285**:** F459-F471, 2003

45. Náray-Fejes-Tóth A, Canessa C, Cleaveland ES, Aldrich G, Fejes-Tóth G: sgk is an aldosterone-induced kinase in the renal collecting duct. Effects on epithelial Na^+ channels. *Journal of Biological Chemistry,* 274**:** 16973-16978, 1999

46. Naray-Fejes-Toth A, Boyd C, Fejes-Toth G: Regulation of epithelial sodium transport by promyelocytic leukemia zinc finger protein. *American Journal of Physiology - Renal Physiology,* 295**:** F18-F26, 2008

47. Kamynina E, Dedonneville C, Dens M, Vandewalle A, Staub O: A novel mouse Nedd4 protein suppresses the activity of the epithelial Na^+ channel. *FASEB Journal,* 15**:** 204-214, 2001

48. Cheval L, Van Huyen JPD, Bruneval P, Verbavatz JM, Elalouf JM, Doucet A: Plasticity of mouse renal collecting duct in response to potassium depletion. *Physiological Genomics,* 19**:** 61-73, 2004

49. Saxena V, Fitch J, Ketz J, White P, Wetzel A, Chanley MA*, et al.*: Whole Transcriptome Analysis of Renal Intercalated Cells Predicts Lipopolysaccharide Mediated Inhibition of Retinoid X Receptor alpha Function. *Scientific Reports,* 9, 2019

50. Spindler B, Mastroberardino L, Custer M, Verrey F: Characterization of early aldosterone-induced RNAs identified in A6 kidney epithelia. *Pflugers Arch,* 434**:** 323-331, 1997

51. Mastroberardino L, Spindler B, Forster I, Loffing J, Assandri R, May A*, et al.*: Ras pathway activates epithelial Na^+ channel and decreases its surface expression in Xenopus oocytes. *Molecular Biology of the Cell,* 9**:** 3417-3427, 1998

52. Mueller JW, Gilligan LC, Idkowiak J, Arlt W, Foster PA: The Regulation of Steroid Action by Sulfation and Desulfation. *Endocrine Reviews,* 36**:** 526-563, 2015

53. Cole GB, Keum G, Liu J, Small GW, Satyamurthy N, Kepe V*, et al.*: Specific estrogen sulfotransferase (SULT1E1) substrates and molecular imaging probe candidates. *Proceedings of the National Academy of Sciences of the United States of America,* 107**:** 6222-6227, 2010

54. Shimada M, Terazawa R, Kamiyama Y, Honma W, Nagata K, Yamazoe Y: Unique properties of a renal sulfotransferase, st1d1, in dopamine metabolism. *Journal of Pharmacology and Experimental Therapeutics,* 310**:** 808-814, 2004

55. Staub O, Loffing J: Mineralocorticoid action in the aldosterone sensitive distal nephron. In: *Seldin and Giebisch's The Kidney - Physiology and Pathophysiology.* 5th Ed. edited by Alpern M, Caplan, M. and Moe, O., London, Academic Press, 2013, pp 1181-1211

56. Funder JW, Pearce PT, Smith R, Smith AI: Mineralocorticoid action: Target tissue specificity is enzyme, not receptor, mediated. *Science,* 242**:** 583-585, 1988

57. Bailey MA, Unwin RJ, Shirley DG: In vivo inhibition of renal 11b-hydroxysteroid dehydrogenase in the rat stimulates collecting duct sodium reabsorption. *Clinical Science,* 101**:** 195-198, 2001

58. Nesterov V, Dahlmann A, Krueger B, Bertog M, Loffing J, Korbmacher C: Aldosterone-dependent and -independent regulation of the epithelial sodium channel (ENaC) in mouse distal nephron. *American Journal of Physiology - Renal Physiology,* 303**:** F1289-F1299, 2012

59. Wu P, Gao Z-X, Zhang D-D, Duan X-P, Terker AS, Lin D-H*, et al.*: Effect of angiotensin II on ENaC in the distal convoluted tubule and in the cortical collecting duct of mineralocorticoid receptor deficient mice. *Journal of the American Heart Association,* 9, 2020

60. Bertog M, Cuffe JE, Pradervand S, Hummler E, Hartner A, Porst M*, et al.*: Aldosterone responsiveness of the epithelial sodium channel (ENaC) in colon is increased in a mouse model for Liddle's syndrome. *Journal of Physiology,* 586**:** 459-475, 2008

61. Nesterov V, Bertog M, Canonica J, Hummler E, Coleman R, Welling PA*, et al.*: Critical role of the mineralocorticoid receptor in aldosterone-dependent and aldosterone-independent regulation of ENaC in the distal nephron. *American Journal of Physiology - Renal Physiology,* 321**:** F257-F268, 2021

62. Bostonjoglo M, Reeves WB, Reilly RF, Velazquez H, Robertson N, Litwack G*, et al.*: 11 beta-hydroxysteroid dehydrogenase, mineralocorticoid receptor, and thiazide-sensitive Na-Cl cotransporter expression by distal tubules. *Journal of the American Society of Nephrology,* 9**:** 1347-1358, 1998

63. Chen LH, Chou CL, Knepper MA: Targeted Single-Cell RNA-seq Identifies Minority Cell Types of Kidney Distal Nephron. *Journal of the American Society of Nephrology,* 32**:** 886-896, 2021

64. Labarca M, Nizar JM, Walczak EM, Dong WX, Pao AC, Bhalla V: Harvest and primary culture of the murine aldosterone-sensitive distal nephron. *American Journal of Physiology - Renal Physiology,* 308**:** F1306-F1315, 2015

65. Assmus AM, Mansley MK, Mullins LJ, Peter A, Mullins JJ: mCCD(c11) cells show plasticity consistent with the ability to transition between principal and intercalated cells. *American Journal of Physiology - Renal Physiology,* 314**:** F820-F831, 2018

66. Guo QS, Wang YQ, Tripathi P, Manda KR, Mukherjee M, Chaklader M*, et al.*: Adam10 mediates the choice between principal cells and intercalated cells in the kidney. *Journal of the American Society of Nephrology,* 26**:** 149-159, 2015

67. Rupprecht R, Reul J, Vansteensel B, Spengler D, Soder M, Berning B*, et al.*: Pharmacological and functional characterization of human mineralocorticoid and glucocorticoid receptor ligands. *Eur J Pharmacol-Molec Pharmacol Sect,* 247**:** 145-154, 1993

68. Young MJ, Moussa L, Dilley R, Funder JW: Early inflammatory responses in experimental cardiac hypertrophy and fibrosis: Effects of 11 beta-hydroxysteroid dehydrogenase inactivation. *Endocrinology,* 144**:** 1121-1125, 2003

Tables

Table 1. Differential analysis of gene expression following acute corticosteroid treatment of $mCCD_{cl1}$ cells.

Experimental conditions compared	Upregulated genes	Downregulated genes
Vehicle *vs.* Aldosterone	8	1
Vehicle *vs.* Corticosterone	0	0
Vehicle *vs.* CBX + Corticosterone	123	78
Aldosterone *vs.* CBX + Corticosterone	64	7
Corticosterone *vs.* CBX + Corticosterone	82	22

Number of genes up or downregulated in each contrast made of experimental condition according to the thresholds on minimum $\log_2$ fold change (1) and maximum false discovery rate (0.05).

Table 2. Differentially expressed genes in $mCCD_{cl1}$ cells following aldosterone treatment.

Upregulated genes (Veh *vs.* Aldo)			
Gene Symbol	**Gene Name**	**Log_2FC**	**FDR**
Zbtb16	Zinc finger and BTB domain-containing 16	3.2	6.0×10^{-12}
Sgk1	Serum and glucocorticoid-regulated kinase 1	2.9	0.0001
Tslp	Thymic stromal lymphopoietin	2.1	0.0477
Rasd1	Ras related dexamethasone-induced 1	2.1	9.4×10^{-10}
Gm16178	N/A	1.6	0.0007
Sult1d1	Sulfotransferase family 1D, member 1	1.1	3.2×10^{-14}
Gm43305	N/A	1.1	0.0002
Defb1	Defensin beta 1	1.0	0.0005
Downregulated transcripts (Veh *vs.* Aldo)			
Gene Symbol	**Gene Name**	**Log_2FC**	**FDR**
Gm9694	N/A	-3.0	0.0444

The threshold for False Discovery Rate (FDR) was 0.05 and the Log_2 fold change (Log_2FC) threshold was 1.

Table 3. Differentially expressed genes in $mCCD_{cl1}$ cells following corticosterone treatment, in the absence of 11βHSD2 activity.

Top 15 upregulated annotated genes (Veh *vs.* CBX+cort)			
Gene Symbol	**Gene Name**	**Log_2FC**	**FDR**
Zbtb16	Zinc finger and BTB domain-containing 16	5.7	7.4×10^{-18}
Sgk1	Serum and glucocorticoid-regulated kinase 1	5.6	3.1×10^{-8}
Rasd1	Ras related dexamethasone-induced 1	4.2	7.0×10^{-19}
Hif3a	Hypoxia inducible factor 3, alpha subunit	2.7	1.1×10^{-14}
Sult1a1	Sulfotransferase family 1A, phenol-preferring, member 1	2.7	0.0005
Sult1d1	Sulfotransferase family 1D, member 1	2.6	3.0×10^{-10}
Tsc22d3	TSC22 domain family, member 3	2.5	1.2×10^{-8}
Myom2	Myomesin 2	2.5	0.0031
Htr6	5-Hydroxytryptamine receptor 6	2.4	0.0198
Slco4c1	Solute carrier organic anion transporter family, member 4C1	2.3	0.0012
Tekt4	Tektin 4	2.2	4.1×10^{-5}
Per1	Period circadian clock 1	2.1	5.3×10^{-6}
Abcb5	ATP-binding cassette, sub-family B (MDR/TAP), member 5	2.1	2.4×10^{-11}
Adora2b	Adenosine A2b receptor	2.1	6.4×10^{-9}
Arg2	Arginase type II	2.1	1.3×10^{-12}
All downregulated annotated genes (Veh *vs.* CBX+cort)			
Gene Symbol	**Gene Name**	**Log_2FC**	**FDR**
Hao2	Hydroxyacid oxidase 2	-2.2	6.8×10^{-6}
Lipc	Lipase, hepatic	-1.8	0.0210
Il1f6	Interleukin 1 family, member 6	-1.7	0.0012
Mboat4	Membrane bound O-acyltransferase domain containing 4	-1.5	0.0026
Pabpn1l	Poly(A) binding protein nuclear 1-like	-1.4	8.5×10^{-6}
Sprr2g	Small proline-rich protein 2G	-1.3	0.0348
Prl2c5	Prolactin family 2, subfamily c, member 5	-1.3	0.0305
Gimap1	GTPase, IMAP family member 1	-1.2	0.0364
Id4	Inhibitor of DNA binding 4	-1.2	0.0276

The threshold for false discovery rate (FDR) was 0.05 and the log_2 fold change (Log_2FC) threshold was 1. For clarity only annotated genes are shown, a full list can be found in the supplemental excel file.

Table 4. Validation of isolated primary CD cells by qRT-PCR.

			tdTom population		GFP population			
Tubule-specific target	**Symbol**	**Nephron segment**	**Cq**	**Expression of GOI relative to reference genes (log_{10})**	**Cq**	**Expression of GOI relative to reference genes (log_{10})**	**Cq range of standards**	**Population enriched?**
NHE3	*Slc9a3*	Proximal tubule	30.6 ± 1.2	0.56 ± 0.47	34.4 ± 0.5	-0.91 ± 0.34***	29.3-34.7	tdTom
NKCC2	*Slc12a1*	Loop of Henle	30.3 ± 1.0	-0.03 ± 0.18	32.3 ± 0.8	-3.00 ± 3.81**	26.9-32.4	tdTom
NCC	*Slc12a3*	Distal Convoluted Tubule	30.4 ± 1.3	-0.47 ± 0.10	29.0 ± 0.6	-0.33 ± 0.13	25.1-30.7	-
11βHSD2	*Hsd11b2*	Collecting duct – principal cell	BLD	BLD	25.8 ± 0.7	0.09 ± 0.11	23.6-29.1	GFP
α-ENaC	*Scnn1a*	Collecting duct – principal cell	BLD	BLD	31.2 ± 0.8	-0.10 ± 0.18	29.1-32.8	GFP
ROMK	*Kcnj1*	Collecting duct – principal cell	BLD	BLD	33.7 ± 0.6	-0.02 ± 0.16	32.4-35.1	GFP
Pendrin	*Slc26a4*	Collecting duct – β-intercalated cell	BLD	BLD	30.5 ± 0.8	-0.02 ± 0.14	27.4-33.1	GFP
AE1	*Slc4a1*	Collecting duct – α-intercalated cell	35.4 ± 0.9	-0.48 ± 0.38	34.8 ± 0.7	-0.33 ± 0.29	29.7-35.7	-
V-ATPase β1	*Atp6v1b1*	Collecting duct – α - and β-intercalated cell	BLD	BLD	32.2 ± 0.6	-0.06 ± 0.14	28.4-34.2	GFP
UT-A1	*Slc14a2*	Medullary collecting duct	BLD	BLD	31.9 ± 0.8	0.20 ± 0.22	29.1-35.2	GFP
			tdTom population		**GFP population**			
Reference gene	**Symbol**		**Cq**	**Expression (log_{10})**	**Cq**	**Expression (log_{10})**	**Cq range of standards**	**Population enriched?**
β-actin	*Actb1*	Reference gene	28.7 ± 1.1	-1.13 ± 0.43	27.6 ± 0.7	-0.68 ± 0.27	26.1-30.9	-
18S	*Rn18s*	Reference gene	15.7 ± 1.4	-1.12 ± 0.46	15.6 ± 0.7	-1.13 ± 0.36	13.1-18.2	-

Expression of nephron segment-specific genes in either tdTom-labelled (n = 5) or GFP-labelled (n = 5) populations of cells isolated by FACS. For each gene of interest (GOI), both the Cq (cycle quantification value) and transcript expression relative to the average expression of reference genes (log10) is shown. The range of Cq values detected across the 7-point standards is also shown. The population where the GOI was found to be enriched, determined either by statistical significance of the relative expression (log10) or where one population showed expression within the 7 point standard and the other was below the limit of detection (BLD), is highlighted in the final column. A hyphen denotes no difference in gene expression between tdTom and GFP populations. Statistical significance was determined by unpaired t-test, ** $p < 0.01$, *** $p < 0.001$.

Figures and figure legends

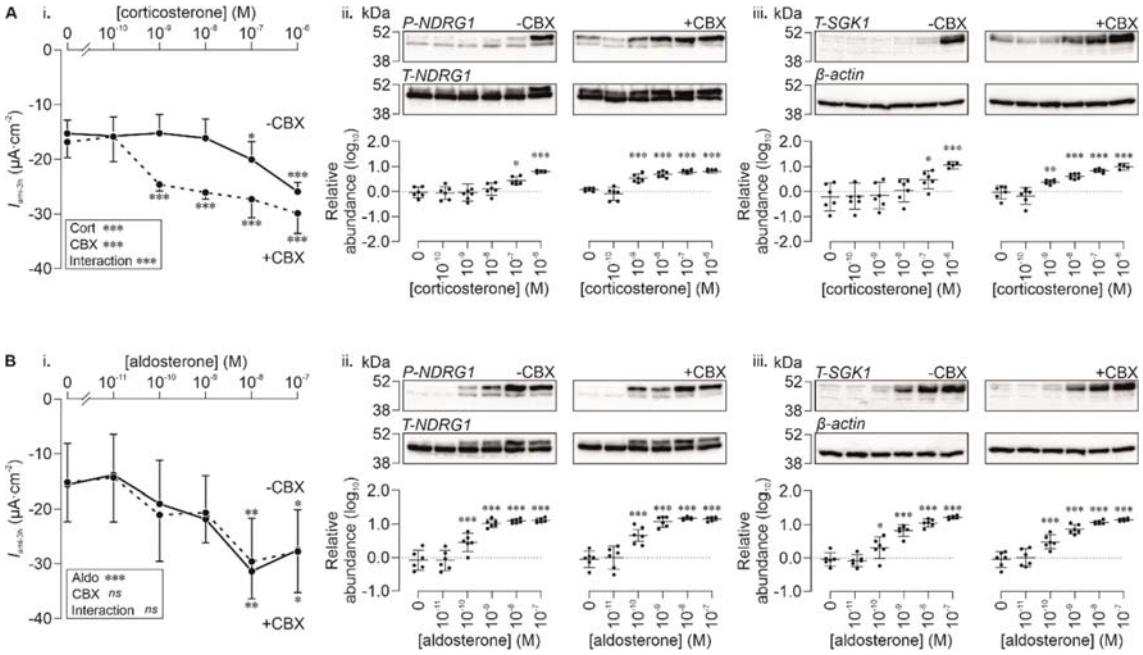

Figure 1. Effects of acute corticosteroids on ENaC-mediated transport and SGK1 activity and expression in mCCD$_{cl1}$ cells. Amiloride-sensitive currents measured from polarised mCCD$_{cl1}$ cells after 3h (I_{ami-3h}) exposure to increasing concentrations of corticosterone (Ai) or aldosterone (Bi) in the absence (-CBX, solid line) or presence (+CBX, dashed line) of carbenoxolone (10 μM, 30 min preincubation), to inhibit 11βHSD2 activity. H_2O was used as vehicle control for CBX, amiloride (10 μM, 10 min) was added following corticosteroid treatment. The activity (ii) and expression (iii) of SGK1 was determined by measuring the abundance of P-NDRG1 or T-SGK1, respectively, in cell lysates following corticosteroid treatment and electrophysiological measurements. These are expressed relative to T-NDRG1 and β-actin, respectively. Upper panels show representative blots and lower panels show densitometric data expressed as a fold change from the control (0) lane ($\log_{10}$). Data are shown as mean ± 95% CI (n = 7). Statistical significance was determined by a two-way ANOVA for the electrophysiological data, with a Dunnett's post-hoc test, and a one-way ANOVA for Western blot data, due to separate blots for – and + CBX, with a Dunnett's post-hoc test.

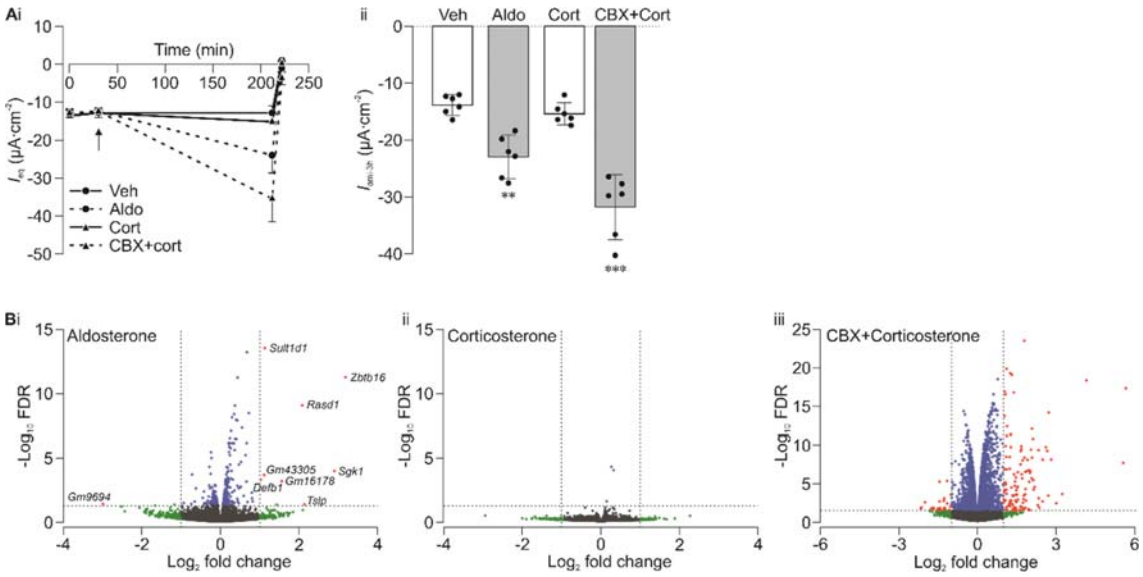

Figure 2. Differentially expressed transcripts in corticosteroid-treated mCCD$_{cl1}$ cells. (Ai) I_{eq} measured from cells treated with either solvent vehicle (Veh), 3 nM aldosterone (Aldo), or 100 nM corticosterone (Cort) for 3 h, arrow indicates addition of corticosteroid. An additional corticosterone group was pre-treated carbenoxolone (CBX) (10 μM, 30 min), all other groups received vehicle control for this period. Amiloride (10 μM) was added to the apical bath for a final 10 min, (ii) shows the amiloride-sensitive current ($I_{ami\text{-}3h}$). Data are shown as mean ± 95% CI (left panel) and as individual points and mean ± 95% CI (right panel). Statistical significance was determined by one-way ANOVA with a Tukey's post-hoc test used to compare groups to vehicle control, $^{**}p<0.01$, $^{***}p< 0.001$. (B) Differentially expressed transcripts are plotted as $\log_2$ fold change versus $-\log_{10}$ false discovery rate (FDR). The horizontal dashed line represents the specified FDR threshold (0.05) and the vertical dashed lines indicate the specified fold change threshold (2) in both positive and negative directions. Each treatment: (Bi) aldosterone, (ii) corticosterone or (iii) CBX+corticosterone, is compared to vehicle-treated control. Points passing only the FDR threshold are shown in green, passing only the fold change threshold are shown in blue and those passing both thresholds are shown in red. Individual transcripts passing both thresholds in aldosterone-treated cells are labelled.

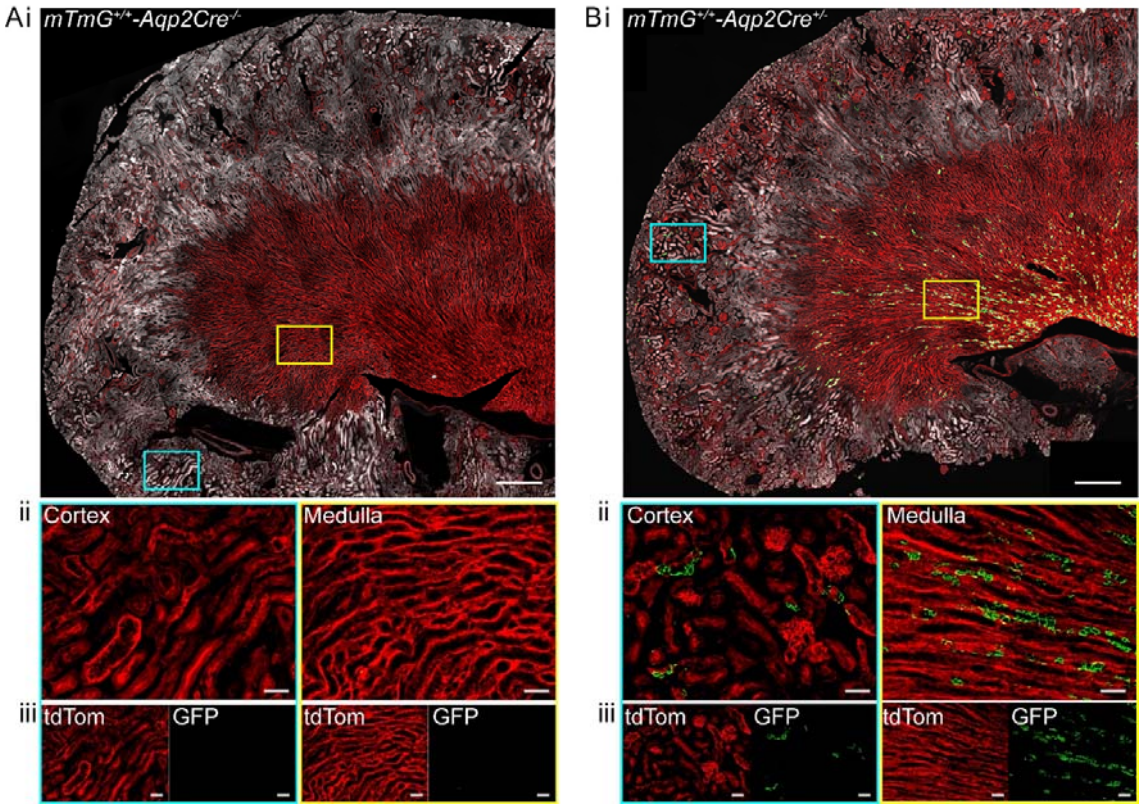

Figure 3. tdTom and GFP expression in kidney sections from mTmG-Aqp2Cre mice. Longitudinal sections of fixed kidneys from adult mTmG$^{+/+}$-Aqp2Cre$^{-/-}$ mice (A) and mTmG$^{+/+}$-Aqp2Cre$^{+/-}$ mice (B) showing tdTom and GFP labelling. (i) Tiled images taken with 40X objective across the section with 488 nm (grey: autofluorescence to show tissue morphology, green: GFP signal) and 555 nm (red: tdTomato signal) excitation light. (ii) Cortex and medullary regions are shown at higher magnification, regions of interest denoted in (i) by cyan and yellow boxes, respectively. (iii) Individual 555 nm and 488 nm channels for (ii) are shown. Scale bars: (i) 500 µm, (ii-iii) 50 µm.

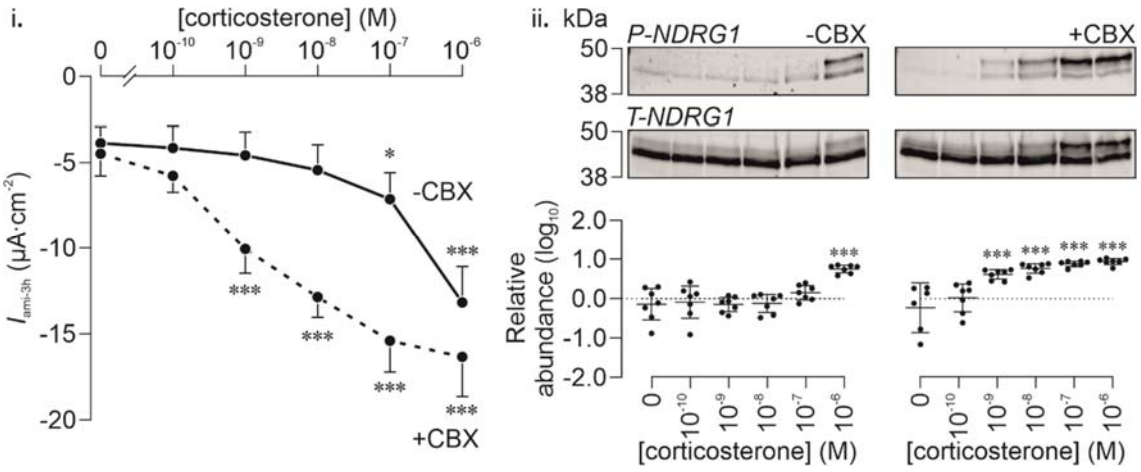

Figure 4. Effects of acute addition of corticosterone on ENaC-mediated transport and SGK1 activity and expression in cultured primary principal cells. (i) Amiloride-sensitive currents were determined in primary principal cells after 3h ($I_{ami\text{-}3h}$) exposure to increasing concentrations of corticosterone in the absence (-CBX) or presence (+CBX) of carbenoxolone (10 μM, 30 min preincubation), to inhibit 11βHSD2 activity. H_2O was used as vehicle control for CBX, amiloride (10 μM, 10 min) was added following corticosteroid treatment. (ii) The activity of SGK1 was determined by measuring the abundance of P-NDRG1 in cell lysates following corticosteroid treatment and electrophysiological measurements, expressed relative to T-NDRG1. Upper panels show representative blots and lower panels show densitometric data expressed as a fold change from the control (0) lane ($\log_{10}$). Data are shown as mean ± 95% CI (n = 7). Statistical significance was determined by a two-way ANOVA for the electrophysiological data and a one-way ANOVA for Western blot data, due to separate blots for – and + CBX, with a Dunnet's post-hoc test, ***p<0.001.

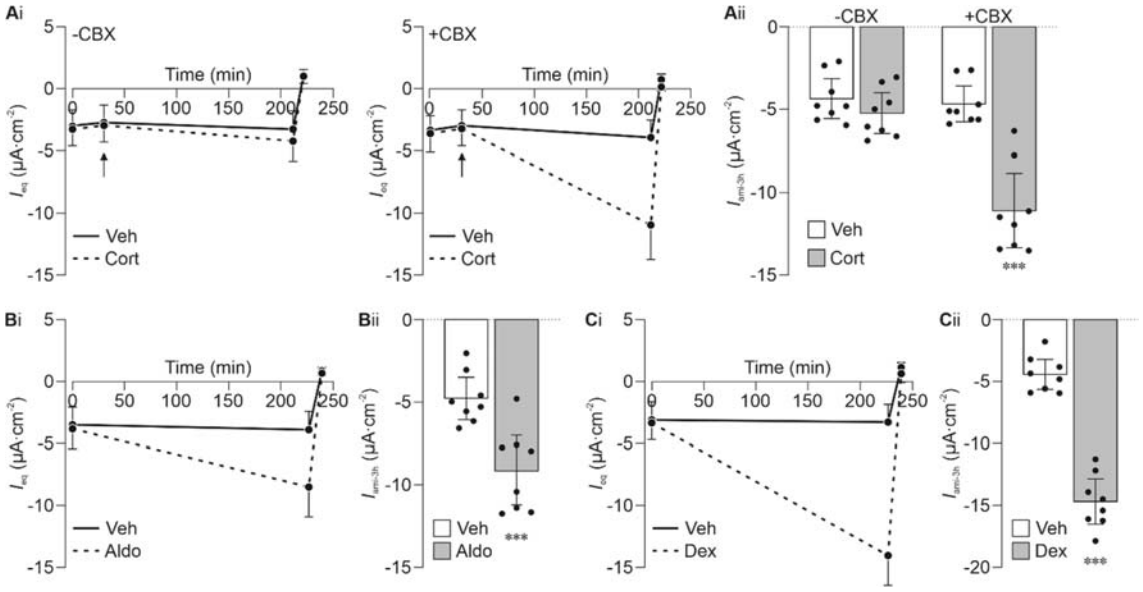

Figure 5. Corticosteroids stimulate ENaC-mediated Na^+ transport in cultured primary principal cells. I_{eq} was measured across polarised monolayers of primary principal cells following treatment with corticosteroids. (A) Cells were pre-incubated with H_2O (-CBX, left) or 10 µM carbenoxolone (+CBX, right) for 30 min. Corticosterone (Cort, 10 nM, dashed line) or solvent vehicle (solid line) was subsequently added for 3 h, arrow denotes addition. (B) Aldosterone (Aldo, 3 nM, dashed line) and (C) dexamethasone (Dex, 100 nM, dashed line), or respective solvent vehicle (solid line), were added to cells for 3 h. In all experiments, amiloride (10 µM) was subsequently applied for 10 min. Data shown in traces (Ai, Bi, Ci) are mean I_{eq} ± 95% CI and in bar graphs (Aii, Bii, Cii) as individual points and mean $I_{ami\text{-}3h}$ ± 95 % CI (n = 8). Statistical significance in (A) was determined by two-way ANOVA and Tukey's post hoc test and in (B) and (C) by unpaired t-test, ***p<0.001.

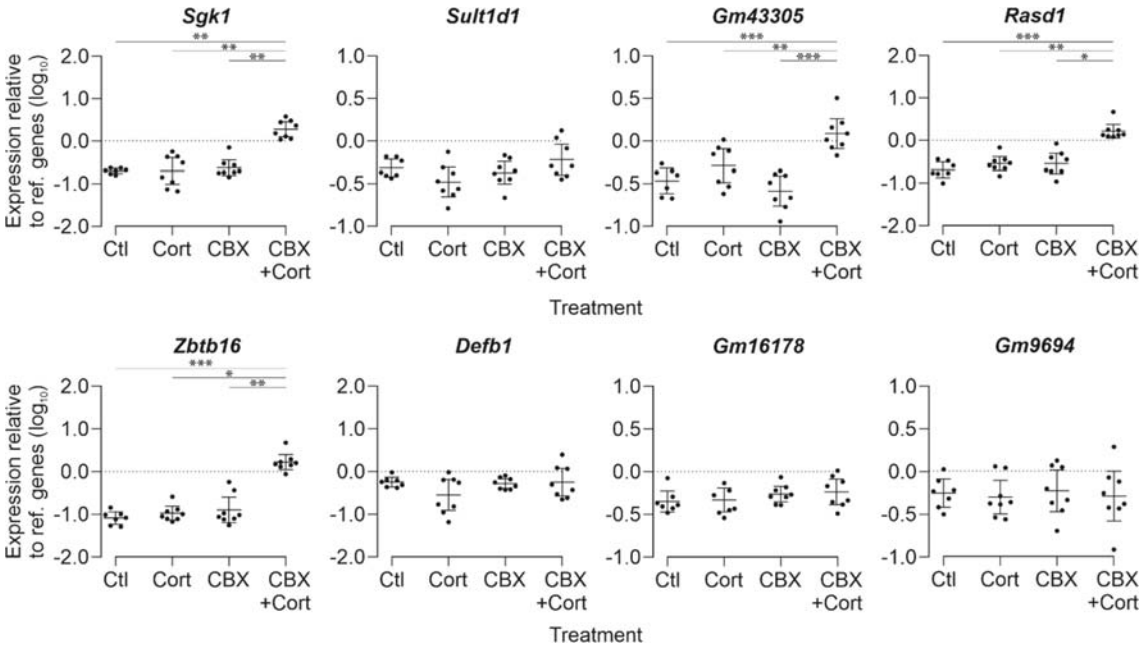

Figure 6. Expression of identified corticosteroid-induced transcripts in primary principal cells treated with corticosterone. Cells were treated with carbenoxolone (CBX) or solvent vehicle for 30 min before addition of corticosterone (Cort, 10 nM) or solvent vehicle for a further 3 h. Amiloride (10 μM) was added for a final 10 min. Transcript expression of GOI is relative to the average expression of reference genes (log_{10}): *Actb1* and *Hprt*. Data are shown as individual points and mean ± 95% CI and GOI is indicated in bold italics above each graph. Statistical significance was determined by one-way ANOVA with Tukey's post-hoc test or Kruskal-Wallis test with Dunn's post-hoc test, where appropriate, *p<0.05, **p<0.01, ***p<0.001.

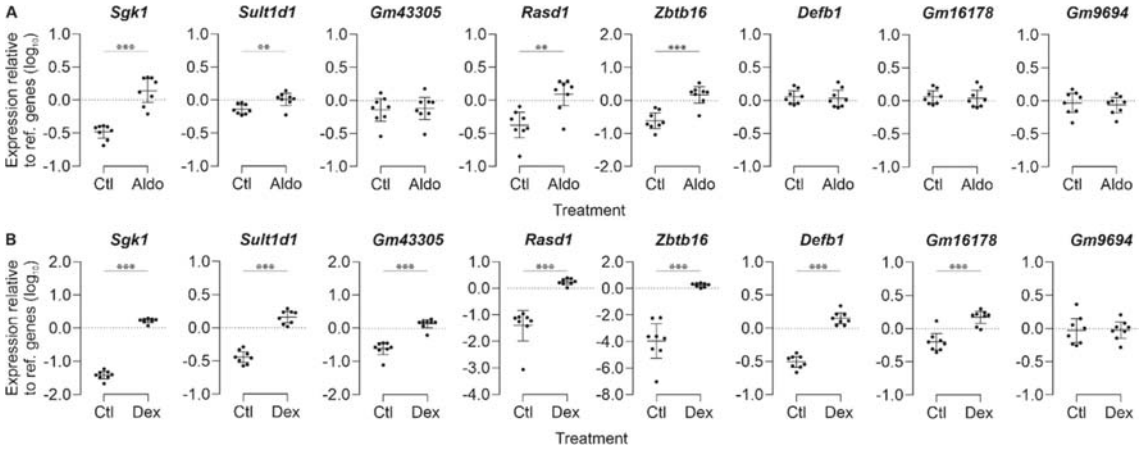

Figure 7. Expression of identified corticosteroid-induced transcripts in primary principal cells treated with aldosterone or dexamethasone. Polarised primary principal cells were treated with either (A) aldosterone (Aldo, 3 nM) or (B) dexamethasone (Dex, 100 nM) for 3 h. Amiloride (10 μM) was added for a final 10 min. Transcript expression of GOI is relative to the average expression of reference genes (log_{10}): *Rn18S* and *Tbp* (Aldo) or *Rn18s*, *Tbp* and *Hprt* (Dex). Data are shown as individual points and mean ± 95% CI and GOI is indicated in bold italics above each graph. Statistical significance was determined by unpaired t-test or Mann-Whitney test, where appropriate, $^{**}p<0.01$, $^{***}p<0.001$.

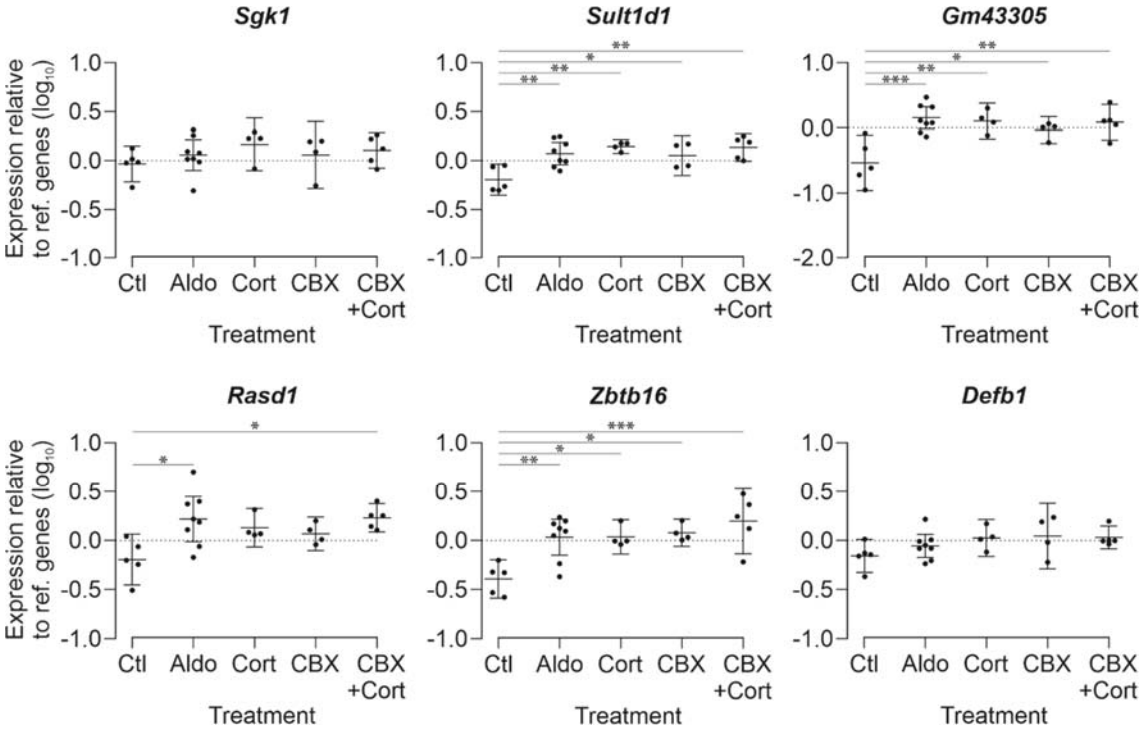

Figure 8. Steroid-induced transcript expression in isolated primary principal cells following acute injection of corticosteroids. Expression of selected target genes were quantified in cells isolated from mT/mG-Aqp2Cre mice 3 h after *ip* injection of solvent vehicle (Ctl), aldosterone (Aldo), corticosterone (Cort), following 8 days *ad lib* access to H_2O. Two further groups were concomitantly treated with carbenoxolone (2.5mg/kg BW/day *po*) for 8 days with subsequent *ip* injection of solvent vehicle (CBX) or corticosterone (CBX+Cort) for 3 h. Target genes were selected from both aldosterone-induced genes identified in the RNA sequencing dataset. Transcript expression of GOI is relative to the average expression of reference genes (log_{10}): *Rn18S* and *Tbp*. Data are shown as individual points and mean ± 95% CI and GOI is indicated in bold italics above each graph. Statistical significance was determined by one-way ANOVA with Tukey's post-hoc test or Kruskal-Wallis test with Dunn's post-hoc test, where appropriate, *p<0.05, **p<0.01, ***p<0.001.

SUPPLEMENTARY

Supplemental Material TOC

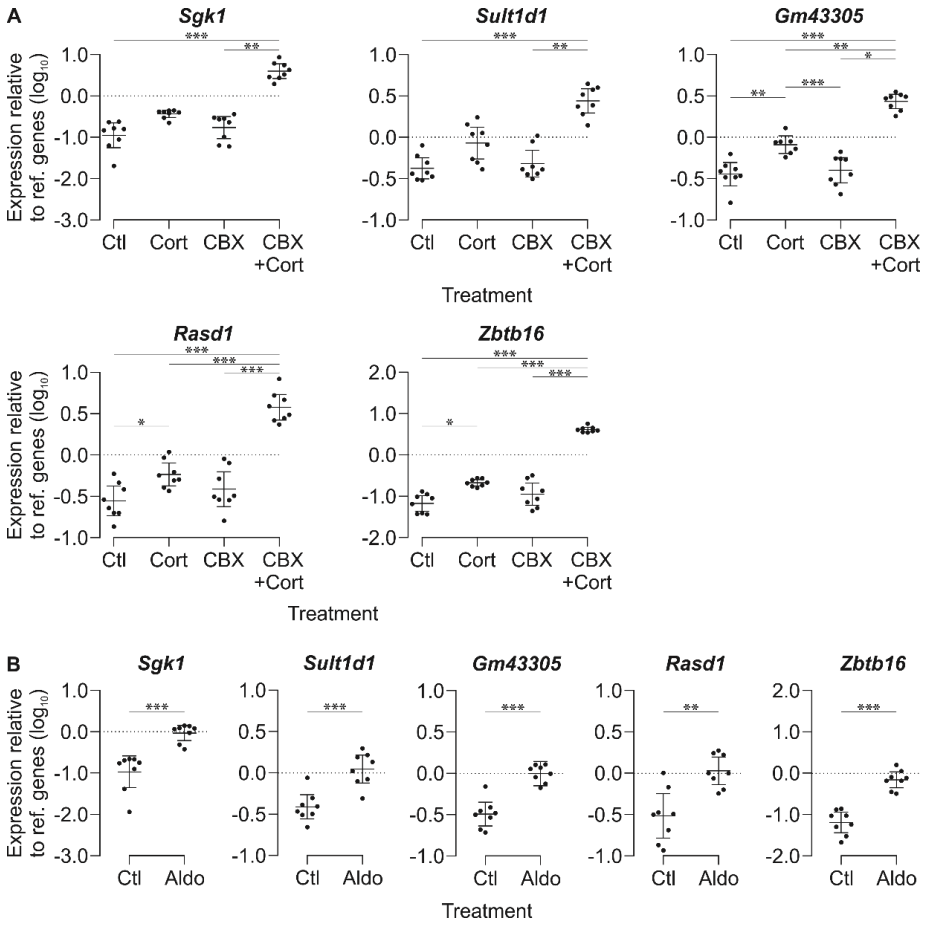

Supplementary Figure 1. Validation of corticosteroid-induced transcripts in mCCD$_{cl1}$ cells. Expression of five identified corticosteroid-induced target transcripts in mCCD$_{cl1}$ cells was quantified by qRT-PCR. (A) Cells were treated with carbenoxolone (CBX) or solvent vehicle for 30 min before addition of corticosterone (Cort, 100 nM) or solvent vehicle for a further 3 h. (B) Cells were treated with aldosterone (Aldo, 3 nM) or solvent vehicle for 3 h. Amiloride (10 µM) was added at the end of all experiments for a final 10 min. Transcript expression of GOI is relative to the average expression of reference genes ($\log_{10}$): *Tbp*, *Rn18S*, *Actb1* and *Hprt*. Data are shown as individual points and mean ± 95% CI and GOI is indicated in bold italics above each graph. Statistical significance was determined in (A) by either one-way ANOVA with Tukey's post-hoc test or Kruskal-Wallis test with Dunn's post-hoc test, where appropriate and in (B) by unpaired t-test or Mann-Whitney test, where appropriate. *p<0.05, **p<0.01, ***p<0.001.

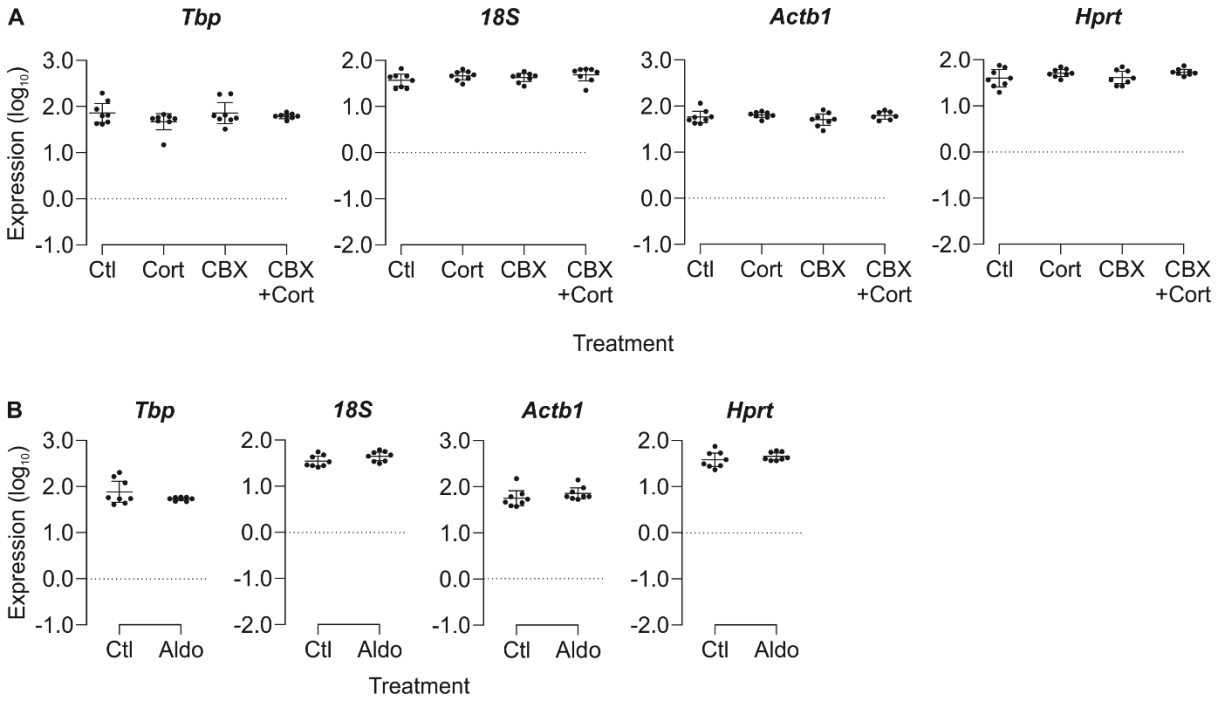

Supplementary Figure 2. Expression of reference genes used for validation of identified corticosteroid-induced transcripts. (A) $mCCD_{cl1}$ cells were treated with carbenoxolone (CBX) or solvent vehicle for 30 min before addition of corticosterone (Cort, 100 nM) or solvent vehicle for a further 3 h. (B) Cells were treated with aldosterone (Aldo, 3 nM) or solvent vehicle for 3 h. Amiloride (10 μM) was added at the end of all experiments for a final 10 min. Data are shown as transcript expression (log_{10}) for each reference gene tested, as individual points and mean ± 95% CI, reference gene is indicated in bold italics above each graph. Statistical significance was determined in (A) by either one-way ANOVA with Tukey's post-hoc test or Kruskal-Wallis test with Dunn's post-hoc test, where appropriate and in (B) by unpaired t-test or Mann-Whitney test, where appropriate.

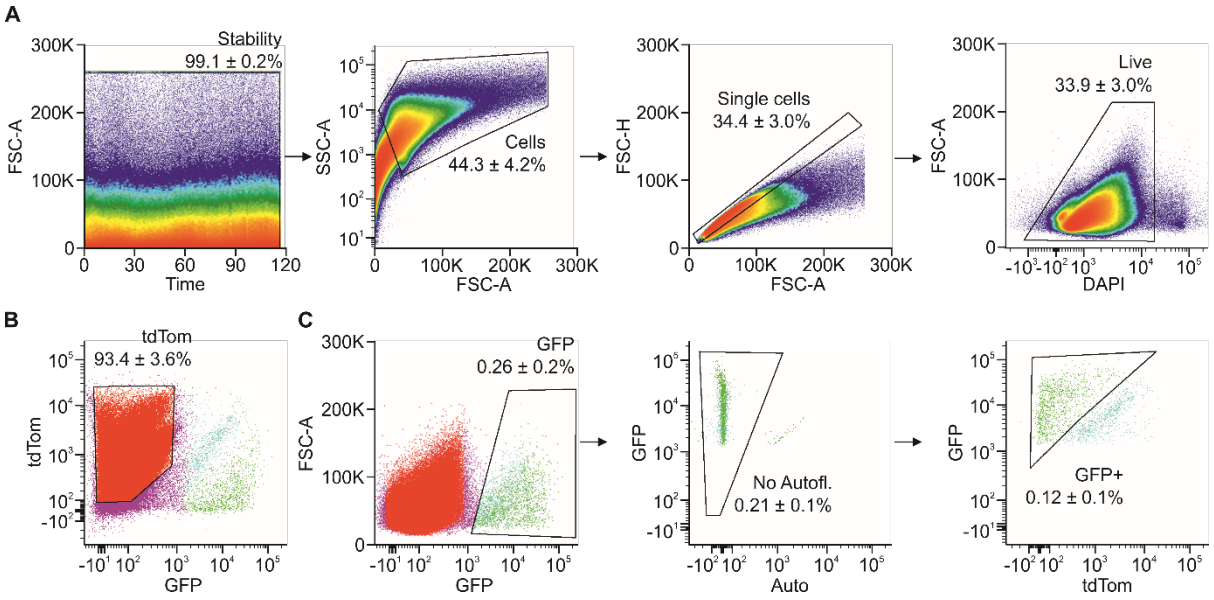

Supplementary Figure 3. Gating strategy for FACS of primary cells into tdTom and GFP labelled populations. (A) Initial gates were applied to identify a stable recording and live, single cells. This population was further gated for (B) tdTom and (C) GFP positive populations. (C) Within the GFP population, a further gate removed any autofluorescence events detected (No Autofl.) and a final gate was added to remove a small sub-population of GFP-tdTom positive cells (GFP+), enabling isolation of a pure GFP positive population.

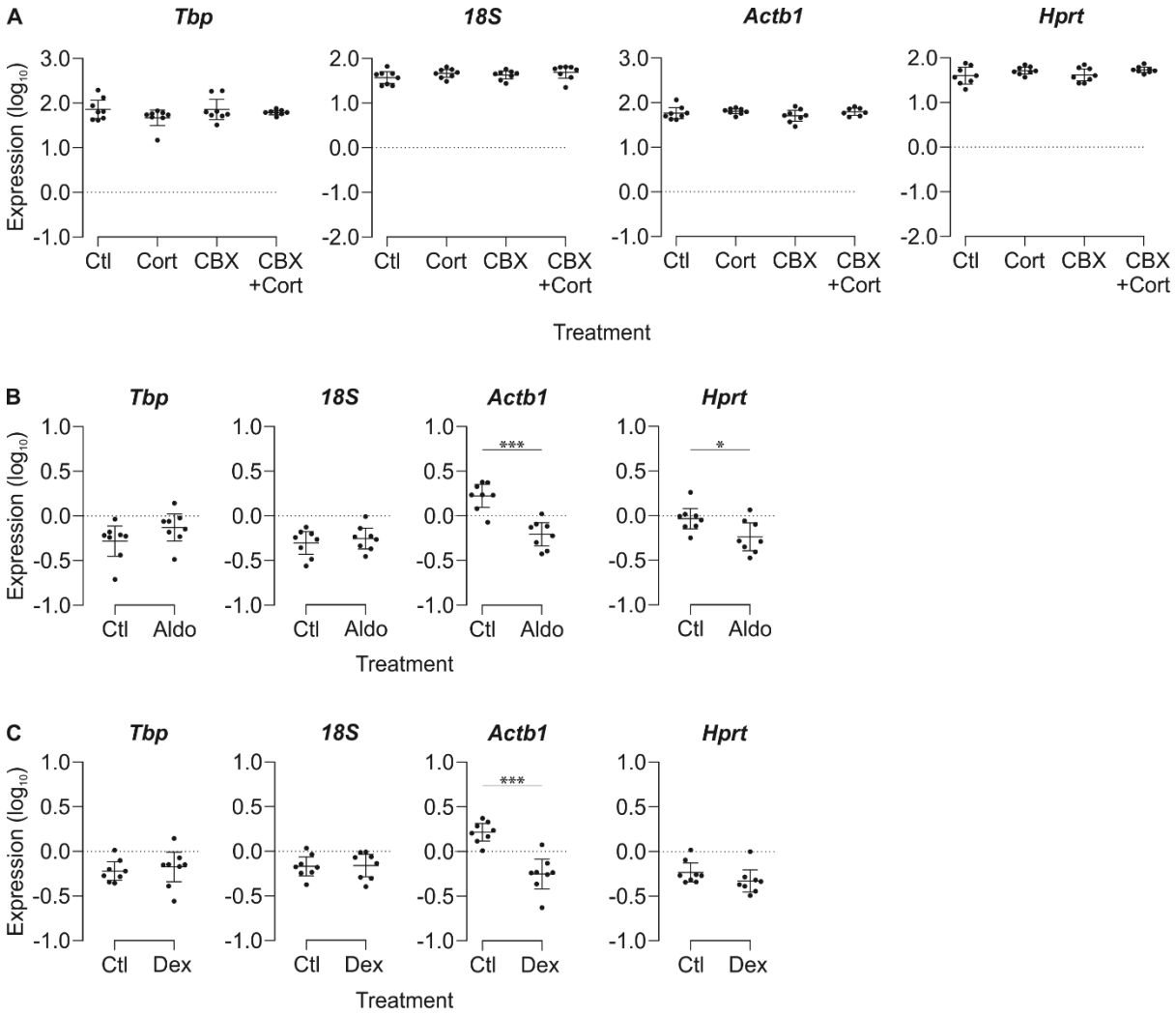

Supplementary Figure 4. Expression of reference genes used for measurement of identified corticosteroid-induced transcripts in primary principal cells. (A) Cultured primary principal cells were treated with carbenoxolone (CBX) or solvent vehicle for 30 min before addition of corticosterone (Cort, 100 nM) or solvent vehicle for a further 3 h. Cells were treated with (B) aldosterone (Aldo, 3 nM), (C) dex (Dex, 100 nM), or their respective solvent vehicle for 3 h. Amiloride (10 μM) was added at the end of all experiments for a final 10 min. Data are shown as transcript expression (log_{10}) for each reference gene tested, as individual points and mean ± 95% CI and reference gene is indicated in bold italics above each graph. Statistical significance was determined in (A) by either one-way ANOVA with Tukey's post-hoc test or Kruskal-Wallis test with Dunn's post-hoc test, where appropriate and in (B) by unpaired t-test or Mann-Whitney test, where appropriate, *p<0.05, ***p<0.001.

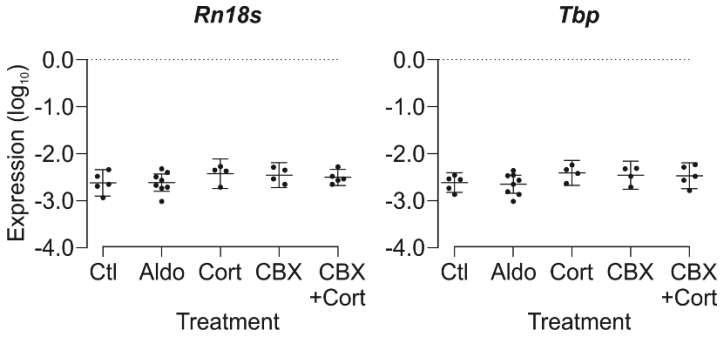

Supplementary Figure 5. Expression of reference genes used for measurement of steroid-induced targets in isolated primary principal cells in mT/mG-Aqp2Cre mice following acute injection of corticosteroids. Expression of reference genes were quantified in cells isolated from mT/mG-Aqp2Cre mice 3 h after *ip* injection of solvent vehicle (Ctl), aldosterone (Aldo), corticosterone (Cort), following 8 days *ad lib* access to H_2O. Two further groups were concomitantly treated with carbenoxolone (2.5mg/kg BW/day *po*) for 8 days with subsequent *ip* injection of solvent vehicle (CBX) or corticosterone (CBX+Cort) for 3 h. Data are shown as transcript expression (log_{10}) for each reference gene tested, as individual points and mean ± 95% CI and reference gene is indicated in bold italics above each graph.